mast cells/basophils [7], neutrophils [8], and NKT cells [9]. In the case of $CD8^+$ T cells, stimulation with the TCR complex leads to the *de novo* expression of CD4 on their surface [10–12]; these cells are targets of HIV-1. Recently, Bernstein *et al.* reported that CD4 is expressed on lymphoid organ-derived and *in vitro*-activated NK cells [13]. It is possible that such CD4-expressing NK cells are also susceptible to HIV-1.

Therefore, in this study we tried to establish a culture system that enables CD4 expression on activated NK cells and allows HIV-1 infection. The expression of CD4 was up-regulated on NK cells when they were activated with rIL-2 and HFWT cells, which selectively stimulate the proliferation of human NK cells [14–16]. Although the activated NK cells were not susceptible to cell-free HIV-1, infection was observed when the activated NK cells were co-cultured with HIV-1-infected T cells. This co-culture system allows us to understand how HIV-1 infects NK cells and how NK cell functions are disrupted in AIDS.

## Results

### CD4 is induced on NK cells by stimulation

We initially induced the expression of CD4 on NK cells *in vitro*. Because HFWT cells selectively stimulate proliferation of human NK cells [14–16], we used them as feeder cells. Freshly isolated cord blood mononuclear cells (CBMC) from HIV-1-seronegative donors were cultured with or without HFWT cells in the presence of rIL-2 for 8 days. Freshly isolated and stimulated CBMC were stained with anti-CD3, -CD4, and -CD56 mAb, and CD4 expression on NK cells was analyzed. Although we could not completely exclude the possibility that a small percentage of resting (freshly isolated) NK cells express CD4 as described previously [3, 13], we detected only background levels of CD4 on the resting NK cells (Fig. 1A, C). CD4 was weakly detected on rIL-2-stimulated NK cells, and the percentage of $CD4^+$ NK cells was greatly augmented among HFWT/rIL-2-stimulated NK cells (Fig. 1A left and 1C). To exclude the possibility of non-specific binding of mAb to the NK cells, we used a different fluorochrome-conjugated anti-CD4 mAb clone (S3.5); we could confirm that the stimulated NK cells do express CD4 on their surface (*i.e.* staining was not due to non-specific binding of the mAb and fluorochrome; Fig. 1B). The percentage of $CD4^+$ NK cells among total NK cells was significantly higher in the HFWT cell/rIL-2-stimulated PBMC and CBMC than in the NK cells or freshly isolated NK cells stimulated with rIL-2 alone (Fig. 1C). Thus, the expression of CD4 was greatly up-regulated on NK cells when they were stimulated with HFWT cells plus rIL-2.

To investigate the kinetics of CD4 expression on NK cells, we determined the percentage and number of $CD4^+$ NK cells after stimulation of CBMC with HFWT cells/rIL-2 or rIL-2 alone. The percentage reached a maximum in the culture with HFWT cells at day 8 (Fig. 2A). The total number of $CD4^+$ NK cells reached a maximum in the culture with HFWT cells around day 13 and was much greater in the HFWT cell-stimulated culture than in the culture stimulated with rIL-2 alone (Fig. 2B). Similar results were obtained from PB NK cells (data not shown). Because there are no significant differences in CD4 expression between cord blood (CB) and PB NK cells, we used mainly CB NK cells in further studies. Both the percentage and number of $CD4^+$ NK cells decreased after the maximum values were obtained. Thus, the percentage and number of $CD4^+$ NK cells rose temporarily after stimulation with HFWT cells and rIL-2.

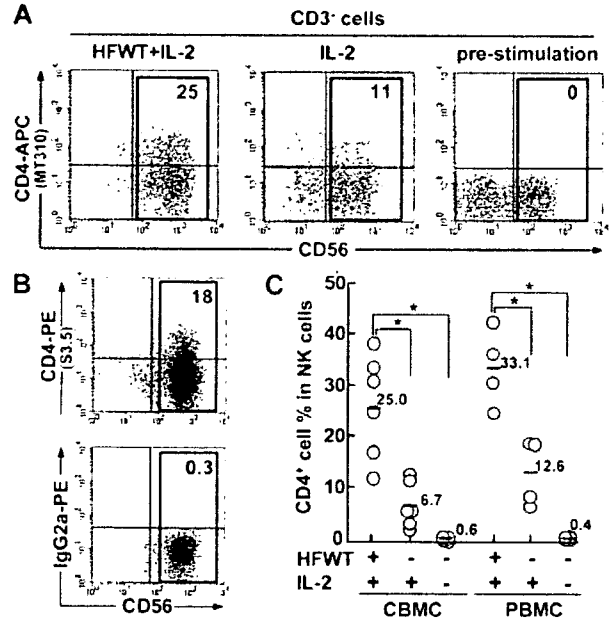


**Figure 1.** Up-regulation of CD4 expression on NK cells following stimulation. (A) CBMC were stimulated with HFWT and rIL-2 or with rIL-2 alone for 8 days. Cells were stained with anti-CD3-PECy7, CD4-APC, and CD56-PE. NK ($CD3^-CD56^+$) cells among the stimulated or freshly isolated CBMC were analyzed for CD4 expression by flow cytometry. Bold squares show total NK cells. Numbers indicate the percentage of $CD4^+$ cells among NK cells. The clone name of the mAb is given in parentheses. (B) CD4 expression on NK cells was analyzed using a PE-conjugated mAb clone different from that used in (A). An isotype control mAb was used as a negative control. (C) Percentages of $CD4^+$ NK cells among resting or stimulated NK cells in CBMC ($n$=6) and PBMC ($n$=4) at day 8. Asterisks show a significant difference. Bars indicate the mean value.

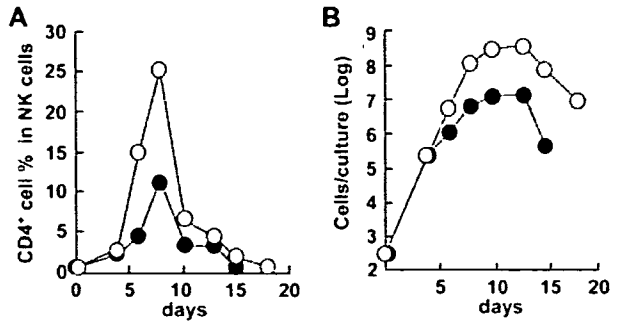


**Figure 2.** Kinetics of CD4 expression on NK cells following stimulation. Time course of changes in $CD4^+$ NK cell frequencies in the total NK cell population (A) and absolute NK cell numbers per culture (B). Representative data from two samples of CBMC are shown. Open and closed circles indicate the HFWT/rIL-2-stimulated culture and rIL-2-stimulated culture, respectively.

## Expression levels of CD4 and HIV-1 co-receptors on NK cells

We next compared expression levels of CD4 on NK cells and helper T cells. $CD4^+$ and $CD4^-$ NK cells were purified from the $CD3^-$ fraction of CBMC cultured with HFWT cells plus rIL-2 (Fig. 3A). To ensure that the same concentrations of mAb and staining conditions were used, we compared the expression level of CD4 between purified $CD4^+$ NK cells and $CD4^+$ T cells in the same culture (fraction b in Fig. 3A). The mean fluorescence of CD4 on $CD4^+$ NK cells was 30 times less than that on $CD4^+$ T cells (Fig. 3B). HIV-1 also needs a co-receptor, CCR5 or CXCR4, on the target cell's surface [17]. Therefore, we next analyzed co-receptor expression on the NK cells. Although resting NK cells were negative or only slightly positive for CCR5 in our flow cytometric analyses and in other reports [18–20], CCR5 was clearly detected on the $CD4^+$ NK cells after stimulation. In contrast, only a low level of CXCR4 expression was detected (Fig. 3C). $CD4^-$ NK cells expressed similar levels of these co-receptors (data not shown). We further attempted to detect CD4 mRNA in the purified $CD4^+$ NK cells by RT-PCR; we detected the mRNA at a low, but significant, level. In contrast, CD4 mRNA was not detected in $CD4^-$ NK cells. In addition, the mRNA of CCR5 and CXCR4 were also detected in the NK cells (Fig. 3D). Thus, although the CD4 expression level was lower on NK cells than on $CD4^+$ T cells, we could confirm that the NK cells express not only CD4 but also HIV-1 co-receptors on their surface.

## $CD4^+$ NK cells are highly activated compared to $CD4^-$ NK cells

To characterize the $CD4^+$ NK cells, we analyzed the phenotype and cytotoxicity of the HFWT cell/rIL-2-stimulated NK cells. Because other researchers have reported that cellular activation up-regulates the expression of CD4 on $CD8^+$ T cells and NK cells [10–13], we initially analyzed the activation of the NK cells. CBMC cultured with HFWT cells plus rIL-2 were analyzed on day 7, and $CD4^+$ and $CD4^-$ NK cells were evaluated in terms of size/granularity (based on FSC/SSC parameters) and expression of the cell surface activation markers HLA-DR and CD25. Size/granularity and the expression of HLA-DR and CD25 were greater for $CD4^+$ NK cells than for $CD4^-$ NK cells (Fig. 4A). Next

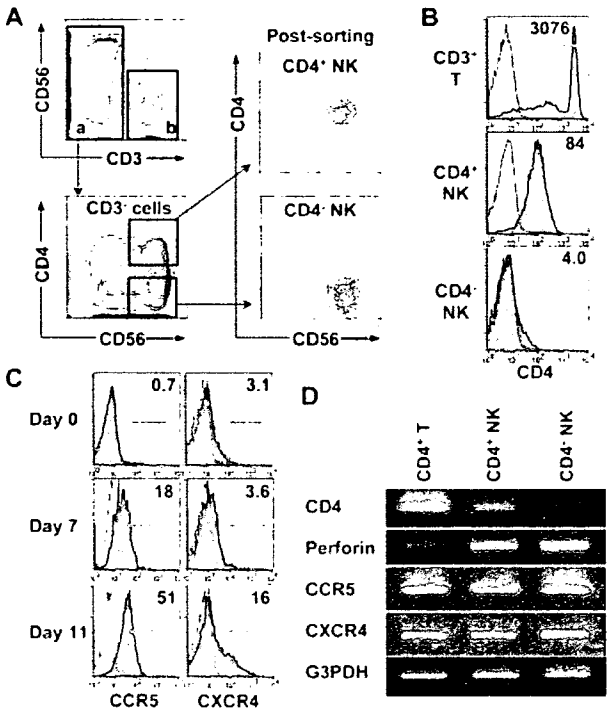


**Figure 3.** Expression of HIV-1 receptors on NK cells. (A) $CD4^+$ and $CD4^-$ NK cells were purified from the HFWT/rIL-2-stimulated CBMC with a cell sorter at day 7. (B) Comparison of CD4 expression on $CD3^+$ T cells (fraction b in A) and the purified NK cell fractions. Thin lines indicate the negative control. Numbers show the mean fluorescence intensity of CD4 on the $CD4^+$ T cells (gray bar) and both NK cell fractions. (C) The expression levels of CCR5 and CXCR4 on freshly isolated CB NK cells (day 0) and $CD4^+$ NK cells (days 7 and 11) were analyzed. The open (white) and gray peaks show the results for isotype-matched control mAb and test mAb, respectively. Numbers indicate the percentage of positive cells. (D) Total RNA was isolated from purified $CD4^+$ T cells, $CD4^+$ NK cells, and $CD4^-$ NK cells on day 7 after stimulation of CBMC and was analyzed by RT-PCR. Perforin and G3PDH were used as positive controls for NK cells and total cells, respectively.

we analyzed expression of some NK receptors and adhesion molecules; the levels of these molecules were similar on $CD4^+$ and $CD4^-$ NK cells (Fig. 4B).

To compare the cytotoxic activity of $CD4^+$ and $CD4^-$ NK cells against K562 cells, we purified $CD4^+$ and $CD4^-$ NK cells with a cell sorter and determined cytotoxicity as described in our previous report [16]. $CD4^+$ NK cells had a level of cytotoxicity similar to $CD4^-$ NK cells (Fig. 4C). These results suggest that $CD4^+$ NK cells were highly activated compared to $CD4^-$ NK cells; however, no significant differences in expression levels of NK receptors and adhesion molecules or cytotoxic activity between $CD4^+$ and $CD4^-$ NK cells were detected.

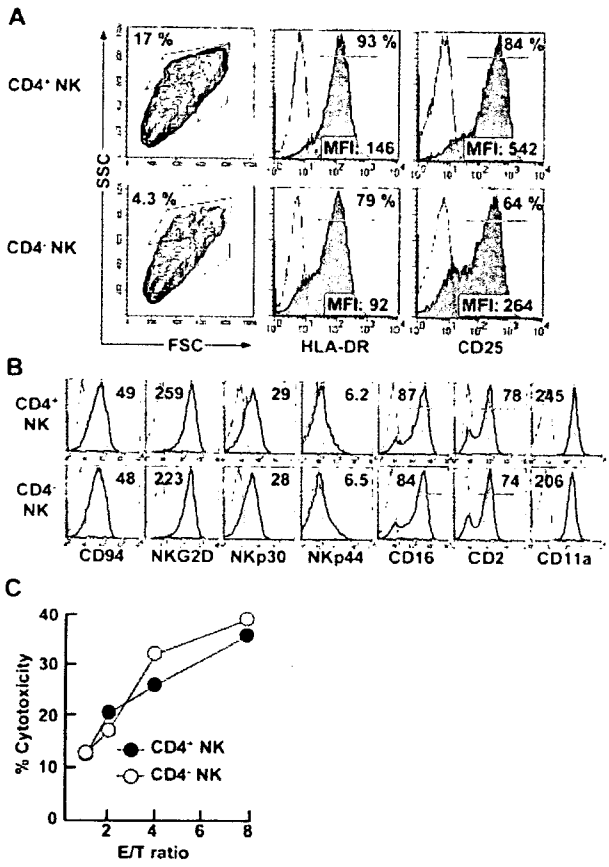


**Figure 4.** Expression of cell surface molecules and activation of $CD4^+$ NK cells. (A) The HFWT/rIL-2-stimulated CBMC were stained with CD3-PECy7, CD56-Alexa 700, CD4-APC, and FITC- or PE-conjugated mAb on day 7. The FSC/SSC profiles and the expression of activation markers on $CD4^+$ and $CD4^-$ NK cells were analyzed. The regions in the FSC/SSC contour blot delineate NK cell blasts. Open histograms show isotype controls. (B) Expression of NK receptors and adhesion molecules on NK cells. Similar results were obtained from at least three samples of CBMC and two samples of PBMC. Numbers in the histograms for CD16 and CD2 are percentages. Numbers in other histograms indicate mean fluorescence intensity. (C) Cytotoxic activity of $CD4^+$ NK cells. $CD4^+$ (closed) and $CD4^-$ (open) NK cells were purified with a cell sorter on day 7. Cytotoxic activity against EGFP-K562 cells was measured by flow cytometry. Representative results of three independent experiments are shown.

## HIV-1 infection of activated NK cells

Because CCR5 was clearly expressed on the $CD4^+$ NK cells (Fig. 3C) and CCR5-tropic HIV-1 is found in primary infections and during all stages of AIDS [17], we exposed CBMC-derived NK cells to HIV-$1_{JR\text{-}FL}$, a CCR5-tropic strain [21]. After 7 days of exposure, we attempted to detect the intracellular HIV-1 core protein p24 by flow cytometry. However, p24 was not detected in NK cells and was only slightly detected in T cells (Fig. 5A, left). Next, to examine the involvement of

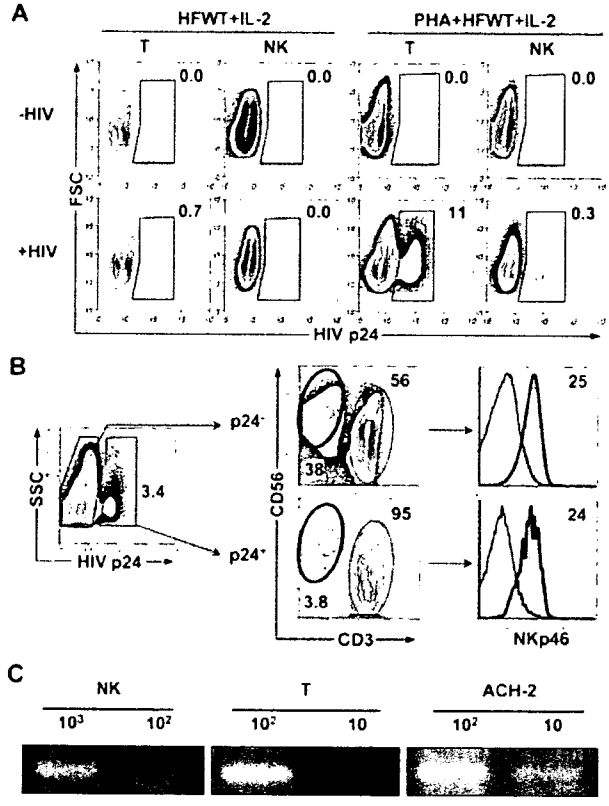


**Figure 5.** HIV-1 infection of NK cells. (A) CBMC were stimulated with HFWT and rIL-2 or HFWT, rIL-2, and PHA for 7 days and further incubated with or without HIV-$1_{JR\text{-}FL}$ for 7 days. Live ($EMA^-$; ethidium monoazide-negative) cells were analyzed for intracellular p24 in NK cell and T cell fractions. The numbers indicate the percentage of $p24^+$ cells. (B) $CD56^+CD3^-$ (bold line) and $CD3^+$ (thin line) cell fractions of $EMA^-$ $p24^+$ or $p24^-$ cells were further analyzed for NKp46 expression. (C) NK cells and T cells were purified from HIV-$1_{JR\text{-}FL}$-exposed PHA/HFWT/rIL-2-stimulated cells by flow cytometry, and DNA was isolated from the sorted cells. PCR analysis was performed to detect the LTR-gag region of HIV-1 proviral DNA. ACH-2 cells, which contain 1 copy of proviral DNA per cell, were used as a positive control. Numbers indicate the cell number per lane. A representative result from at least two experiments is shown.

HIV-1-infected T cells in the infection of NK cells, we added PHA to the culture to improve the efficiency of HIV infection *in vitro*. Subsequently, the cells were exposed to $HIV_{JR\text{-}FL}$. We then detected intracellular p24 not only in T cells but also weakly in the NK cell fraction (Fig. 5A, right). When cultured in the presence of PHA but without $CD4^+$ T cells, NK cells were not susceptible to HIV-1 (data not shown). To exclude the possibility of T cell contamination, the $p24^+$ NK cell fraction was further analyzed for the expression of an NK cell receptor, NKp46, as an NK cell-specific marker [22]. As shown in Fig. 5B, NKp46 was detected in the $p24^+$ NK cell fraction but not in the T cell fraction. In addition, the $p24^+$ NK cell fraction did not express markers for NKT cells (TCR Vβ11) or γδ T cells (TCRγδ) (data not shown). Thus $p24^+CD3^-CD56^+$ cells were certainly NK cells. Furthermore, to confirm that HIV proviral DNA was integrated into the NK cells, we purified NK cells and T cells from the HIV-1-exposed cells using a cell sorter and analyzed HIV-1 proviral DNA by PCR. We detected the proviral DNA not only in T cells but also in the NK cells. The amount of HIV-1 proviral DNA integrated was about 1 copy per 100 NK cells (Fig. 5C). These results suggest that HIV-1 infects NK cells *via* infected T cells.

## Discussion

In this study, we demonstrated that NK cells express CD4 and HIV-1 co-receptors when cultured with IL-2 and HFWT cells, which stimulate human NK cells [14–16]. Moreover, the stimulated NK cells were susceptible to HIV-1 when they were co-cultured with HIV-1-infected T cells.

Recently, Bernstein *et al.* [13] reported that CD4 is expressed on lymphoid organ NK cells and activated PB NK cells. In that report, $CD4^+$ NK cells expressed NK cell receptors and activation markers, and CD4 was not involved in the cytotoxic activity. Furthermore, $CD4^+$ NK cells produce large amounts of IFN-γ and TNF-α and migrate to a natural ligand of CD4, IL-16. In this study, we further demonstrated that CD4-expressing NK cells express HIV-1 co-receptors and are susceptible to HIV-1.

Expression of CCR5 is important for HIV-1 infection, because CCR5-tropic HIV-1 is found in primary infections and during all stages of AIDS [17]. In this study, activated NK cells expressed CCR5 after being stimulated (Fig. 3C, D), as described in a previous paper [23]. In other reports, CCR5 was expressed on resting $CD16^-$ NK cells but only at low levels on $CD16^+$ NK cells [18, 20]. In the present study, the expression of CCR5 was not due to the selective proliferation of $CD16^-$ NK cells, as the stimulated NK cells clearly expressed CD16 (Fig. 4B). Expression of CCR5 and activation of NK cells have also been reported in HIV-1-infected patients: Kottilil *et al.* found that immune activation during HIV-1 infection induced an up-regulation of CCR5 expression on NK cells of HIV-1-infected patients [24], while Fogli *et al.* reported that NK cells express activation markers such as HLA-DR and CD69 [25]. Our results confirm that immune activation induces the expression of CCR5 on human NK cells. In contrast, CXCR4 levels were reported to be low on activated NK cells [26].

Because $CD4^+$ NK cells clearly expressed CCR5 on their surface, we tried to infect HFWT cell/rIL-2-activated NK cells with $HIV\text{-}1_{JR\text{-}FL}$. However, cell-free HIV-1 could not infect the NK cells (Fig. 5A left). As described in other reports, soluble anti-HIV-1 factors, such as CC-chemokines [27, 28], might have suppressed susceptibility to cell-free HIV-1. On the other hand, HIV-1 infection of NK cells was observed when CBMC were stimulated under the same culture conditions with PHA to allow HIV-1 infection of $CD4^+$ T cells. The percentage of intracellular HIV-1 p24 was much lower in NK cells than in T cells (Fig. 5A right). The differences between NK cells and T cells in susceptibility to HIV-1 might be caused by the differences in the expression levels of CD4 on these cells; in macrophages/monocytes the expression level of CD4 correlates, at least in part, with sensitivity to HIV-1 [29]. However, NK cells were certainly positive for HIV-1, because $p24^+$ $CD3^-CD56^+$ cells were also positive for the NK cell-selective marker NKp46 (Fig. 5B), and proviral DNA was detected by PCR analysis (Fig. 5C).

HIV-1 infection of HHV-6-infected NK cell clones [30] and primary NK cells [3] has been reported. However, no relationship between the activation of NK cells and expression of CD4 was described in these reports. Only after maximal activation might NK cells be susceptible to HIV-1 infection *in vivo* on the basis of CD4 and CCR5 and/or CXCR4 surface expression. Specifically, it is possible that CD4-expressing NK cell clones were activated through HHV-6 infection. The primary NK cells might be activated and infected by HIV-1 *via* already infected cells, such as T cells and macrophages in the lymphoid organs. However, because HIV-1 proviral DNA was not detected in PB NK cells from viremic patients [4], HIV-1 infection of NK cells is controversial. Still, it is possible that HIV-1 infects NK cells under physiological conditions. $CD56^{bright}$ NK cells in lymph nodes are activated by T cell-derived IL-2 [31]. In addition, CD4 is expressed on NK cells in lymphoid organs of seronegative donors [13]. It is thought that NK cells in lymphoid organs may also express CD4 in HIV-1-infected patients. Furthermore, it has been reported that activated NK cells and $CD4^+$ T cells directly interact *via* co-stimulatory molecules [32] and that activated NK cells directly target the HIV-1-infected $CD4^+$ T cells that down-regulate MHC class I expression [33, 34]. Based on the present study and other reports, we speculate that

when $CD4^+$ NK cells encounter HIV-1-infected cells in lymphoid organs, they become susceptible to HIV-1 *via* direct contact with the infected cells. NK cells may be activated to kill HIV-1-infected cells or suppress viral replication; however, such NK cells may be targets of HIV-1 *in vivo*. The offensive and defensive battles between HIV-1 and NK cells under physiological conditions must be further revealed to better understand the pathogenesis of AIDS.

## Materials and methods

### Cells and culture conditions

All blood samples in this study were collected from HIV-1-seronegative donors after obtaining informed consent based on a protocol approved by an Institutional Review Board. CBMC and PBMC were separated by density-gradient centrifugation with Ficoll. NK cells in CBMC or PBMC were cultured with HFWT cells (Cell-Medicine Inc., Japan) as described in our previous reports [14–16]. Briefly, CBMC and PBMC were cultured with irradiated HFWT cells in RPMI 1640 medium (Sigma-Aldrich Inc., St. Louis, MO) supplemented with 10% autologous plasma with rIL-2 (200 U/mL). PHA (10 ng/mL; Sigma) was added to activate T cells. HFWT cells were maintained in DMEM (Sigma) supplemented with 10% heat-inactivated FBS. ACH-2 [35] and EGFP-K562 cells were cultured in RPMI 1640 medium supplemented with 10% FBS.

### Flow cytometry

Cells were stained with the following mAb: CD2-FITC, CD11a-PE, CD56-APC (allophycocyanin) and -PECy5, NKp46-PE, NKp30-PE, NKG2D-PE, HIV-1 p24-FITC, and HLA-DR-FITC from Beckman Coulter (Fullerton, CA); CD3-PECy7 from e-Bioscience (San Diego, CA); CD3-PE and CD4-PE from Caltag (Burlingame, CA); CD4-APC and CXCR4-PE from Dako cytomation (Glostrup, Denmark); and CD16-FITC, CD25-PE, CD56-PE, -Alexa Fluor 700, and CCR5-FITC from BD Pharmingen (San Diego, CA). After staining, cells were washed with staining medium and then resuspended in washing medium. Intracellular HIV-1 p24 was detected as described elsewhere [36]. After a wash, the cells were analyzed with an LSR II flow cytometer (BD Bioscience, San Jose, CA). Cell size and internal granularity were analyzed with forward scatter (FSC) and side light scatter (SSC), respectively [37]. Cell sorting was performed on a JSAN flow cytometer (Bay Bioscience, Japan). The purity of each sorted fraction was >98%. Data were analyzed with CellQuest (BD Bioscience) or FlowJo (Tree Star, San Carlos, CA) software.

### Cytotoxicity assay

The cytotoxicity of NK cells toward EGFP-K562 cells was measured by flow cytometry with propidium iodide (PI) as described previously [16]. Briefly, 50-μL aliquots of EGFP-K562 cells ($1 \times 10^5$ cells/mL) were placed in 5-mL round-bottomed tubes, and 400 μL of two-fold serially diluted effector cells was added. Effector alone was used as a negative control. After a 6-h incubation at 37°C, 50 μL of 20 μg/mL PI was added and incubated for an additional 15 min. Target cells in FSC vs. SSC dot plots were gated, and GFP and PI were measured using an LSR II flow cytometer (Bay Bioscience, Japan). Cytotoxic activity was calculated as follows: $A/(A+B) \times 100-C$ (%), where A is the percentage of $PI^+EGFP^+$ cells, B is the percentage of $PI^-GFP^+$ cells at each E/T ratio, and C is the percentage of spontaneous $PI^+$ cells without effector cells ($A/(A+B) \times 100$ (%) at E/T ratio =0).

### Virus and infection

pJR-FL [38] (kindly provided by Dr. Y. Koyanagi, Kyoto University) was introduced into HEK 293T cells with Lipofectamin 2000 (Invitrogen) as described in the instruction manual. The culture supernatant was harvested 48 h and 72 h after transfection and stocked as a viral solution at –80°C until use. A 1/10 volume of the viral solution (final concentration of p24, 30–40 ng/mL) was added to the cell culture ($1 \times 10^6$ cells/mL) and incubated for 7 days.

### PCR analysis

Total RNA was extracted with Trizol reagent (Invitrogen) for reverse transcription (RT)-PCR. First-strand cDNA was synthesized with a random primer and AMV reverse transcriptase and then amplified with Ex Taq (Takara, Japan). Total DNA was extracted to detect HIV-1 proviral DNA by PCR [7]. Primer sequences were as follows:

CD4: 5′-GCAGTGGCGAGCTGTGGT [10], 5′-GAGGAGGCGAACAGGAGG; Perforin: 5′-ATGTAACCCGGGCCAAAGTCA, 5′-GTGCCGTAGTTGGAGATAAGC [39]; CCR5: 5′-CGTCTCTCCCAGGAATCATCTTTAC, 5′-TTGAGTCCGTGTCACAAGCCC [40]; CXCR4: 5′-TGACTCCATGAAGGAACCCTG, 5′-CTTGGCCTCTGACTGTTGGTG [41]; G3PDH: 5′-TGAAGGTCGGAGTCAACGGATTTGGT, 5′-CATGTGGGCCATGAGGTCCACCAC; HIV-1 LTR-gag: 5′-GGCTAACTAGGGAACCCACTG [42], 5′-CTTATTACTGACGCTTCTGC [43].

### Statistical analysis

The statistical significance of differences was determined using the Student's *t*-test. *p* values less than 0.05 were defined as statistically significant.

**Acknowledgements:** We are grateful to Dr. K. Matsui and his coworkers (Fukuda Hospital, Kumamoto, Japan) for providing cord blood and Prof. Y. Koyanagi for providing the pJR-FL plasmid [38]. ACH-2 cells [35] were obtained from the National Institutes of Health AIDS Research and Reference Reagent Program (Division of AIDS, National Institute of Allergy and Infectious Diseases, National Institutes of Health, Bethesda, MD). This work was supported in part by Health and Labour Sciences Research Grants from the Ministry of Health, Labour, and Welfare of Japan (H16-AIDS-003 and H19-AIDS-003 to S. O. and S. S.).

 

## References


1 **Cooper, M. A., Fehniger, T. A. and Caligiuri, M. A.,** The biology of human natural killer-cell subsets. *Trends Immunol.* 2001. **22:** 633–640.

2 **Fauci, A. S., Mavilio, D. and Kottilil, S.,** NK cells in HIV infection: paradigm for protection or targets for ambush. *Nat. Rev. Immunol.* 2005. **5:** 835–843.

3 **Valentin, A., Rosati, M., Patenaude, D. J. A., Hatzakis, L., Kostrikis, G., Lazanas, M., Wyvill, K. M. *et al.*,** Persistent HIV-1 infection of natural killer cells in patients receiving highly active antiretroviral therapy. *Proc. Natl. Acad. Sci. USA* 2002. **99:** 7015–7020.

4 **Mavilio, D., Benjamin, J., Daucher, M., Lombardo, G., Kottilil, S., Planta, M. A., Marcenaro, E. *et al.*,** Natural killer cells in HIV-1 infection: dichotomous effects of viremia on inhibitory and activating receptors and their functional correlates. *Proc. Natl. Acad. Sci. USA* 2003. **100:** 15011–15016.

5 **Patterson, S. and Knight, S. C.,** Susceptibility of human peripheral blood dendritic cells to infection by human immunodeficiency virus. *J. Gen. Virol.* 1987. **68:** 1177–1181.

6 **Lusso, P., Garzino-Demo, A., Crowley, R. W. and Malnati, M. S.,** Infection of γ/δ T lymphocytes by human herpesvirus 6: transcriptional induction of CD4 and susceptibility to HIV infection. *J. Exp. Med.* 1995. **181:** 1303–1310.

7 **Li, Y., Li, L., Wadley, R., Reddel, S. W., Qi, J. C., Archis, C., Collins, A. *et al.*,** Mast cells/basophils in the peripheral blood of allergic individuals who are HIV-1 susceptible due to their surface expression of CD4 and the chemokine receptors CCR3, CCR5, and CXCR4. *Blood* 2001. **97:** 3484–3490.

8 **Biswas, P., Mantelli, B., Sica, A., Malnati, M., Panzeri, C., Saccani, A., Hasson, H. *et al.*,** Expression of CD4 on human peripheral blood neutrophils. *Blood* 2003. **101:** 4452–4456.

9 **Motsinger, A., Haas, D. W., Stanic, A. K., Van Kaer, L., Joyce, S. and Unutmaz, D.,** CD1d-restricted human natural killer T cells are highly susceptible to human immunodeficiency virus 1 infection. *J. Exp. Med.* 2002. **195:** 869–879.

10 **Yang, L. P., Riley, J. L., Carroll, R. G., June, C. H., Hoxie, J., Patterson, B. K., Ohshima, Y. *et al.*,** Productive infection of neonatal $CD8^+$ T lymphocytes by HIV-1. *J. Exp. Med.* 1998. **187:** 1139–1144.

11 **Kitchen, S. G., Korin, Y. D., Roth, M. D., Landay, A. and Zack, J. A.,** Costimulation of naive $CD8^+$ lymphocytes induces CD4 expression and allows human immunodeficiency virus type 1 infection. *J. Virol.* 1998. **72:** 9054–9060.

12 **Flamand, L., Crowley, R. W., Lusso, P., Colombini-Hatch, S., Margolis, D. M. and Gallo, R. C.,** Activation of $CD8^+$ T lymphocytes through the T cell receptor turns on CD4 gene expression: implications for HIV pathogenesis. *Proc. Natl. Acad. Sci. USA* 1998. **95:** 3111–3116.

13 **Bernstein, H. B., Plasterer, M. C., Schiff, S. E., Kitchen, C. M., Kitchen, S. and Zack, J. A.,** CD4 expression on activated NK cells: ligation of CD4 induces cytokine expression and cell migration. *J. Immunol.* 2006. **177:** 3669–3676.

14 **Harada, H., Saijo, K., Watanabe, S., Tsuboi, K., Nose, T., Ishiwata, I. and Ohno, T.,** Selective expansion of human natural killer cells from peripheral blood mononuclear cells by the cell line, HFWT. *Jpn. J. Cancer Res.* 2002. **93:** 313–319.

15 **Harada, H., Watanabe, S., Saijo, K., Ishiwata, I. and Ohno, T.,** A Wilms' tumor cell line, HFWT, can greatly stimulate proliferation of both $CD56^+$ human natural killer cells and their novel precursors in blood mononuclear cells. *Exp. Hematol.* 2004. **32:** 614–621.

16 **Harada, H., Suzu, S., Ito, T. and Okada, S.,** Selective expansion and engraftment of human $CD16^+$ NK cells in NOD/Scid mice. *Eur. J. Immunol.* 2005. **35:** 3599–3609.

17 **Berger, E. A., Murphy, P. M. and Farber, J. M.,** Chemokine receptors as HIV-1 coreceptors: roles in viral entry, tropism, and disease. *Annu. Rev. Immunol.* 1999. **17:** 657–700.

18 **Campbell, J. J., Qin, S., Unutmaz, D., Soler, D., Murphy, K. E., Hodge, M. R., Wu, L. *et al.*,** Unique subpopulations of $CD56^+$ NK and NK-T peripheral blood lymphocytes identified by chemokine receptor expression repertoire. *J. Immunol.* 2001. **166:** 6477–6482.

19 **Inngjerdingen, M., Damaj, B. and Maghazachi, A. A.,** Expression and regulation of chemokine receptors in human natural killer cells. *Blood* 2001. **97:** 367–375.

20 **Berahovich, R. D., Lai, N. L., Wei, Z., Lanier, L. L. and Schall, T. J.,** Evidence for NK cell subsets based on chemokine receptor expression. *J. Immunol.* 2006. **177:** 7833–7840.

21 **Koyanagi, Y., Miles, S., Mitsuyasu, R. T., Merrill, J. E., Vinters, H. V. and Chen, I. S.,** Dual infection of the central nervous system by AIDS viruses with distinct cellular tropisms. *Science* 1987. **236:** 819–822.

22 **Pessino, A., Sivori, S., Bottino, C., Malaspina, A., Morelli, L., Moretta, L., Biassoni, R. *et al.*,** Molecular cloning of NKp46: a novel member of the immunoglobulin superfamily involved in triggering of natural cytotoxicity. *J. Exp. Med.* 1998. **188:** 953–960.

23 **Nieto, M., Navarro, F., Perez-Villar, J. J., del Pozo, M. A., Gonzalez-Amaro, R., Mellado, M., Frade, J. M. *et al.*,** Roles of chemokines and receptor polarization in NK-target cell interactions. *J. Immunol.* 1998. **161:** 3330–3339.

24 **Kottilil, S., Shin, K., Planta, M., McLaughlin, M., Hallahan, C. W., Ghany, M., Chun, T. W. *et al.*,** Expression of chemokine and inhibitory receptors on natural killer cells: effect of immune activation and HIV viremia. *J. Infect. Dis.* 2004. **89:** 1193–1198.

25 **Fogli, M., Costa, P., Murdaca, G., Setti, M., Mingari, M. C., Moretta, L., Moretta, A. *et al.*,** Significant NK cell activation associated with decreased cytolytic function in peripheral blood of HIV-1-infected patients. *Eur. J. Immunol.* 2004. **34:** 2313–2321.

26 **Beider, K., Nagler, A., Wald, O., Franitza, S., Dagan-Berger, M., Wald, H., Giladi, H. *et al.*,** Involvement of CXCR4 and IL-2 in the homing and retention of human NK and NK T cells to the bone marrow and spleen of NOD/SCID mice. *Blood* 2003. **102:** 1951–1958.

27 **Fehniger, T. A., Herbein, G., Yu, H., Para, M. I., Bernstein, Z. P., O'Brien, W. A. and Caligiuri, M. A.,** Natural killer cells from $HIV\text{-}1^+$ patients produce C-C chemokines and inhibit HIV-1 infection. *J. Immunol.* 1998. **161:** 6433–6438.

28 **Oliva, A., Kinter, A. L., Vaccarezza, M., Rubbert, A., Catanzaro, A., Moir, S., Monaco, J. *et al.*,** Natural killer cells from human immunodeficiency virus (HIV)-infected individuals are an important source of CC-chemokines and suppress HIV-1 entry and replication *in vitro*. *J. Clin. Invest.* 1998. **102:** 223–231.

29 **Kedzierska, K., Crowe, S. M., Turville, S. and Cunningham, A. L.,** The influence of cytokines, chemokines and their receptors on HIV-1 replication in monocytes and macrophages. *Rev. Med. Virol.* 2003. **13:** 39–56.

30 **Lusso, P., Malnati, M. S., Garzino-Demo, A., Crowley, R. W., Long, E. O. and Gallo, R. C.,** Infection of natural killer cells by human herpesvirus 6. *Nature* 1993. **362:** 458–462.

31 **Fehniger, T. A., Cooper, M. A., Nuovo, G. J., Cella, M., Facchetti, F., Colonna, M. and Caligiuri, M. A.,** $CD56^{bright}$ natural killer cells are present in human lymph nodes and are activated by T cell-derived IL-2: a potential new link between adaptive and innate immunity. *Blood* 2003. **101:** 3052–3057.

32 **Zingoni, A., Sornasse, T., Cocks, B. G., Tanaka, Y., Santoni, A. and Lanier, L. L.,** Cross-talk between activated human NK cells and $CD4^+$ T cells *via* OX40-OX40 ligand interactions. *J. Immunol.* 2004. **173:** 3716–3724.

33 **Bonaparte, M. I. and Barker, E.,** Killing of human immunodeficiency virus-infected primary T-cell blasts by autologous natural killer cells is dependent on the ability of the virus to alter the expression of major histocompatibility complex class I molecules. *Blood* 2004. **104:** 2087–2094.

34 **Vieillard, V., Strominger, J. L. and Debre, P.,** NK cytotoxicity against $CD4^+$ T cells during HIV-1 infection: a gp41 peptide induces the expression of an NKp44 ligand. *Proc. Natl. Acad. Sci. USA* 2005. **102:** 10981–10986.

35 **Folks, T. M., Clouse, K. A., Justement, J., Rabson, A., Duh, E., Kehrl, J. H. and Fauci, A. S.,** Tumor necrosis factor alpha induces expression of human immunodeficiency virus in a chronically infected T-cell clone. *Proc. Natl. Acad. Sci. USA* 1989. **86:** 2365–2368.

36 **Mascola, J. R., Louder, M. K., Winter, C., Winter, C., Prabhakara, R., De Rosa, S. C., Douek, D. C. *et al.*,** Human immunodeficiency virus type 1 neutralization measured by flow cytometric quantitation of single-round infection of primary human T cells. *J. Virol.* 2002. **76:** 4810–4821.

37 **Munz, C., Dao, T., Ferlazzo, G., de Cos, M. A., Goodman, K. and Young, J. W.,** Mature myeloid dendritic cell subsets have distinct roles for activation and viability of circulating human natural killer cells. *Blood.* 2005. **105:** 266–273.


 

38 **Koyanagi, Y., Miles, S., Mitsuyasu, R. T., Merrill, J. E., Vinters, H. V. and Chen, I. S.**, Dual infection of the central nervous system by AIDS viruses with distinct cellular tropisms. *Science* 1987. **236:** 819–822.

39 **Koga, T., Harada, H., Shi, T. S., Okada, S., Suico, M. A., Shuto, S. and Kai, H.**, Hyperthermia suppresses the cytotoxicity of NK cells *via* down-regulation of perforin/granzyme B expression. *Biochem. Biophys. Res. Commun.* 2005. **337:** 1319–1323.

40 **Yi, Y., Rana, S., Turner, J. D., Gaddis, N. and Collman, R. G.**, CXCR-4 is expressed by primary macrophages and supports CCR5-independent infection by dual-tropic but not T-tropic isolates of human immunodeficiency virus type 1. *J. Virol.* 1998. **72:** 772–777.

41 **Naif, H. M., Li, S., Alali, M., Sloane, A., Wu, L., Kelly, M., Lynch, G. *et al.***, CCR5 expression correlates with susceptibility of maturing monocytes to human immunodeficiency virus type 1 infection. *J. Virol.* 1998. **72:** 830–836.

42 **Naif, H. M., Chang, J., Ho-Shon, M., Li, S. and Cunningham, A. L.**, Inhibition of human immunodeficiency virus replication in differentiating monocytes by interleukin 10 occurs in parallel with inhibition of cellular RNA expression. *AIDS Res. Hum. Retroviruses* 1996. **12:** 1237–1245.

43 **Zack, J. A., Arrigo, S. J., Weitsman, S. R., Go, A. S., Haislip, A. and Chen, I. S.**, HIV-1 entry into quiescent primary lymphocytes: molecular analysis reveals a labile, latent viral structure. *Cell* 1990. **61:** 213–222.

 

Available online at www.sciencedirect.com
ScienceDirect
Cancer Letters 257 (2007) 206–215
CANCER Letters
www.elsevier.com/locate/canlet

# Dehydroxymethylepoxyquinomicin (DHMEQ) therapy reduces tumor formation in mice inoculated with Tax-deficient adult T-cell leukemia-derived cell lines

Takeo Ohsugi [a,*], Toshio Kumasaka [b], Seiji Okada [c], Takaomi Ishida [d], Kazunari Yamaguchi [e], Ryouichi Horie [f], Toshiki Watanabe [d], Kazuo Umezawa [g]

[a] *Division of Microbiology and Genetics, Center for Animal Resources and Development, Institute of Resource Development and Analysis, Kumamoto University, 2-2-1 Honjo, Kumamoto 860-0811, Japan*
[b] *Department of Human Pathology, Juntendo University Graduate School of Medicine, 2-1-1 Hongo, Bunkyo-ku, Tokyo 113-8421, Japan*
[c] *Division of Hematopoiesis, Center for AIDS Research, Kumamoto University, 2-2-1 Honjo, Kumamoto 860-0811, Japan*
[d] *Laboratory of Tumor Cell Biology, Department of Medical Genome Sciences, Graduate School of Frontier Sciences, The University of Tokyo, 4-6-1 Shirokanedai, Minato-ku, Tokyo 108-8639, Japan*
[e] *Department of Safety Research on Blood and Biologics, National Institute of Infectious Diseases, Gakuen 4-7-1, Musashimurayama-shi, Tokyo 208-0011, Japan*
[f] *Department of Hematology, Faculty of Medicine, Kitasato University, 1-15-1 Sagamihara, Kanagawa 228-8555, Japan*
[g] *Department of Applied Chemistry, Faculty of Science and Technology, Keio University, 3-14-1 Hiyoshi, Kohoku-ku, Yokohama 223-0061, Japan*

Received 23 February 2007; received in revised form 20 July 2007; accepted 23 July 2007

**Abstract**

Adult T-cell leukemia (ATL) is an aggressive neoplasm caused by human T-cell leukemia virus type I (HTLV-I), which induces nuclear factor-κB (NF-κB), a molecule central to the ensuing neoplasia. The NF-κB inhibitor dehydroxymethylepoxyquinomicin (DHMEQ) has been shown to inhibit NF-κB activation in Tax-expressing HTLV-I-infected cells. In this study, we used NOD/SCID β2-microglobulin$^{null}$ mice to show that intraperitoneal inoculation with Tax-deficient ATL cell lines caused rapid death, whereas DHMEQ-treated mice survived. Furthermore, DHMEQ treatment after subcutaneous inoculation inhibited the growth of transplanted ATL cells. These results demonstrate that DHMEQ has therapeutic efficacy on ATL cells, regardless of Tax expression.


*Keywords:* HTLV-I; ATL; DHMEQ; NF-κB; NOD/SCID β2-microglobulin$^{null}$ mice

*Abbreviations:* ATL, adult T-cell leukemia; HTLV-I, human T-cell leukemia virus type I; DHMEQ, dehydroxymethylepoxyquinomicin; NK, natural killer; SCID, severe combined immunodeficiency; NOD/SCID β2m$^{null}$ mice, non-obese diabetic/severe combined immunodeficiency β2-microglobulin knockout mice; NF-κB, nuclear factor-κB.

* Corresponding author. Tel.: +81 96 373 6549; fax: +81 96 373 6552.
*E-mail address:* ohsugi@gpo.kumamoto-u.ac.jp (T. Ohsugi).

0304-3835/$ - see front matter © 2007 Elsevier Ireland Ltd. All rights reserved.
doi:10.1016/j.canlet.2007.07.017

## 1. Introduction

Adult T-cell leukemia (ATL) is a mature T-cell malignancy caused by human T-cell leukemia virus type I (HTLV-I) infection [1,2]. A minor proportion of HTLV-I-infected carriers develop ATL after a long latency period. However, almost 1000 cases of ATL are diagnosed each year in Japan, no accepted curative therapy for ATL exists, and patients progress to death with a mean survival time of 13 months [3]. ATL patients retain poor prognosis mainly because of resistance to conventional, high-dose, or combination chemotherapy treatment [4]. Therefore, development of novel anti-ATL therapies is greatly needed.

Tax, a 40 kDa protein encoded by the pX region of HTLV-I viral genome activates nuclear factor-κB (NF-κB) by stimulating the activity of the IκB kinase (IKK), which in turn leads to phosphorylation and degradation of IκBα [5,6]. NF-κB is then released from IκBα and translocates to the nucleus where it transactivates various genes encoding cytokines, chemokines and anti-apoptotic proteins [7]. However, NF-κB also may be activated in primary ATL cells and some ATL-derived cell lines that lack viral expression [7–9]. These facts show that Tax-independent mechanisms for constitutive NF-κB activation are present in ATL cells. Regardless of Tax expression, constitutive activation of NF-κB in ATL cells is required for ATL cell growth and survival [7]. Thus, blocking the NF-κB pathway may be a key strategy for the treatment of ATL patients [10,11].

The NF-κB inhibitor, dehydroxymethylepoxyquinomicin (DHMEQ), inhibits activation of NF-κB by preventing nuclear translocation of p65, an NF-κB subunit [12–14]. DHMEQ has already shown potential for inducing apoptosis in prostate cancer, thyroid cancer, pancreatic cancer, multiple myeloma and breast cancer [15–20]. We recently reported that DHMEQ strongly inhibits constitutively activated NF-κB in both ATL-derived cell lines and in primary cultures of ATL cells from patients, inducing apoptosis in these cells at concentrations that do not affect the viability of peripheral blood mononuclear cells [9]. We also observed that DHMEQ induces apoptosis in the Tax-expressing HTLV-I-infected cell lines MT-2 and HUT-102 and inhibits nuclear translocation of the p65 subunit in vitro and in vivo [21,22]. However, we could not evaluate the effects of DHMEQ on the Tax-deficient ATL-derived cell lines TL-Om1 and MT-1 in vivo, because these cells did not grow in severe combined immunodeficiency (SCID) mice in which natural killer (NK) cell activity had been eliminated (NK-free SCID mice) [21].

In this study, we establish a mouse model of ATL using non-obese diabetic (NOD)/SCID and β2-microglobulin knockout (NOD/SCID $\beta2m^{null}$) mice that have low NK cell activity and additionally lack β2-microglobulin (β2m), the light chain of the MHC class I molecule [23]. We inoculated these mice intraperitoneally or subcutaneously with either TL-Om1 or MT-1 and evaluated the effect of DHMEQ treatment in vivo. Mice injected with TL-Om1 or MT-1 cells intraperitoneally but not treated with DHMEQ died soon thereafter from tumor and infiltrative leukemic cell growth, whereas DHMEQ-treated mice survived and showed a decreased rate of inoculated cell infiltration. In the subcutaneous model, DHMEQ induced apoptosis and inhibited the growth of TL-Om1 cells transplanted at the injection site.

## 2. Materials and methods

### 2.1. Cell lines

Four HTLV-I-infected T-cell lines, TL-Om1 [24], MT-1 [2], MT-2 [25] and HUT-102 [1], were maintained at 37 °C in 5% $CO_2$ in RPMI 1640 medium supplemented with 10% fetal bovine serum, 100 U/ml of penicillin and 100 μg/ml of streptomycin. TL-Om1 and MT-1 are leukemic T-cell lines derived from patients with ATL. MT-2 is an HTLV-I-transformed T-cell line established by an in vitro co-culture protocol. HUT-102 was established from a patient originally diagnosed with cutaneous T-cell lymphoma which was later considered a lymphoma type ATL. The clonal origin of this cell line is unclear, and can no longer be determined. An HTLV-I-negative T-cell line, MOLT-4, was maintained in RPMI 1640 supplemented with 10% fetal bovine serum at 37 °C in 5% $CO_2$ and the antibiotics listed above. All cells lines were passaged twice a week.

### 2.2. Characterization of HTLV-I-infected cell lines

To analyze cell cultures for the presence of Tax mRNA, total RNA from cells was extracted using an RNA extraction kit (Qiagen, Valencia, CA) and treated with 10 U DNase I (Takara Bio, Tokyo, Japan) for 30 min at 37 °C. Reverse transcriptase polymerase chain reaction (RT-PCR) was performed using a one-step RNA PCR kit (Takara Bio) with a set of primers for the Tax mRNA [26].

To analyze cell cultures for the presence of Tax protein, samples containing 50 μg of total protein from cell lysates were electrophoresed and transferred to a polyvinylidene difluoride membrane (Atto, Tokyo, Japan). Western blot analysis was carried out to detect Tax protein in each cell line as described [22].

To evaluate viral release into the supernatant, culture samples were taken 3 days after passage. Cell culture medium was centrifuged at 1200*g* for 10 min at 4 °C. Supernatants were then examined for the presence of the HTLV-I p19 antigen using an enzyme-linked immunosorbent assay (ELISA) according to the manufacturer's protocol (Zeptomatrix, Buffalo, NY).

For evaluation of NF-κB activity, the cells ($5 \times 10^6$) were centrifuged at 200*g* for 5 min at 4 °C and washed with cold phosphate-buffered saline and nuclear extracts were subsequently prepared using a nuclear extraction kit (Active Motif, Carlsbad, CA). DNA-binding activity of NF-κB p65 was then measured using microplate-based ELISAs according to the manufacturer's protocol (TransAM NF-κB p65 Transcription Factor Assay kit; Active Motif). Absorbance at 450 nm was determined in each well using a microplate reader (Bio-Rad, Richmond, CA).

### 2.3. Chemicals

Racemic DHMEQ was synthesized as described [13], dissolved in DMSO and subsequently diluted in culture medium to a final concentration of <0.1%.

### 2.4. Nuclear staining to determine apoptosis in vitro

Cells ($1 \times 10^6$) were cultured with 20 or 40 μg/ml of DHMEQ for 48 h. Cells treated with the same concentrations of DMSO solvent without DHMEQ served as controls. Morphologic examination of cells was performed using a phase contrast microscope (CK40: Olympus, Tokyo, Japan). Cells were stained with Hoechst 33342 (Calbiochem, San Diego, CA) and stained apoptotic nuclei were calculated as reported [21,22].

### 2.5. Measurement of NF-κB activity in cells treated with DHMEQ

TL-Om1 or MT-1 cells ($5 \times 10^6$) were cultured with 20 or 40 μg/ml DHMEQ for 16 h. The HTLV-I-uninfected T-cell line, MOLT-4, served as a control. Nuclear and cytoplasmic fractions were then prepared using a nuclear extraction kit according to the manufacturer's protocol (Active Motif). NF-κB activity in nuclear and cytoplasmic fractions was determined by measuring the DNA-binding activity of p65, as described above, and was expressed as a percentage of the binding measured in control cells that were not treated with DHMEQ. The relative ratio of nuclear to cytoplasmic p65 was calculated from the absorbance value of nucleus divided by that of cytoplasm.

### 2.6. Mice

Non-obese diabetic (NOD)/severe combined immunodeficiency (SCID) and β2-microglobulin knockout (NOD/SCID $\beta2m^{null}$) mice were obtained from The Jackson Laboratory (Bar Harbor, ME). The mice were maintained under specific pathogen-free conditions in laminar-flow benches at 22 ± 2 °C with a 12 h light/dark cycle. Mice were fed sterilized (γ-irradiated) pellets and received acidified drinking water (pH 2.5–3.0) *ad libitum*. All procedures involving animals and their care were approved by the animal care committee of Kumamoto University in accordance with Institutional and Japanese government guidelines for animal experiments.

### 2.7. Administration of DHMEQ to NOD/SCID $\beta2m^{null}$ mice injected intraperitoneally with TL-Om1 or MT-1 cells

TL-Om1 or MT-1 cells ($5 \times 10^7$) were washed three times with phosphate-buffered saline and introduced by intraperitoneal injection into 7- to 10-week-old NOD/SCID $\beta2m^{null}$ mice that had been pretreated 1 day earlier with 2 Gy irradiation. DHMEQ was dissolved in 0.5% carboxymethyl cellulose (vehicle) to a final concentration of 1.2 mg/ml. DHMEQ (12 mg/kg) or vehicle was administered intraperitoneally on day 0 of cell inoculation and three times a week thereafter for 5 weeks. Mice surviving for 5 weeks after cell inoculation were autopsied and tumor formation was assessed.

### 2.8. Histology

Organs were fixed in 10% neutral-buffered formalin immediately after removal, embedded in paraffin, cut into 4 μm sections, and stained with hematoxylin and eosin.

### 2.9. PCR analysis of genomic DNA

To detect HTLV-I proviral sequences, 0.5 μg of genomic DNA extracted from tumors or various organs was subjected to PCR analysis [21,22]. Oligonucleotide primers for *tax* and for the human *β-globin* genes (control) were used and PCR was performed as described [21,22].

### 2.10. Administration of DHMEQ to NOD/SCID $\beta2m^{null}$ mice injected with TL-Om1 subcutaneously

DHMEQ was dissolved in 0.5% carboxymethyl cellulose (vehicle) to a final concentration of 1.2 mg/ml. TL-Om1 cells ($5 \times 10^7$) were washed three times with phosphate-buffered saline and introduced by subcutaneous injection into the post-auricular region of 7- to 10-week-old NOD/SCID $\beta2m^{null}$ mice that had been pretreated 1 day earlier with 2 Gy irradiation. DHMEQ

(12 mg/kg) or vehicle was administered by intraperitoneal injection on day 0 of cell inoculation and three times a week thereafter for 5 weeks. Both tumor size and body weight were measured weekly. Tumor volume was calculated according to the formula: $a^2 \times b \times 0.5$, where $a$ and $b$ are the smallest and largest diameters, respectively.

### 2.11. Detection of apoptosis in vivo

Animals were sacrificed 5 weeks after cell inoculation. Gross tumors were immediately fixed in 10% neutral-buffered formalin, appropriately cut and then embedded in paraffin. The tissues were sectioned to 4 μm thickness and stained with hematoxylin and eosin. Apoptosis in tissue sections was examined by TUNEL (terminal deoxynucleotidyl transferase-mediated deoxyuridine triphosphate nick end-labeling) assay using the *in situ* Apoptosis Detection kit (R&D systems, Minneapolis, MN) according to the manufacturer's instructions.

### 2.12. Statistical analysis

Statistical analysis was performed using Fisher's exact probability test and Student's $t$-test. Statistical significance was defined as $P < 0.05$.

## 3. Results

### 3.1. Characterization of HTLV-I-associated cell lines

As expected, MT-2 and HUT-102 expressed significant amounts of Tax mRNA and protein (Fig. 1a). MT-1 cells expressed the HTLV-I Tax transcript, but we were unable to detect Tax protein (Fig. 1a, lower panel). TL-Om1 cells did not express detectable amounts of Tax at either mRNA or protein levels. To assess virus release in these cell lines, we analyzed for the presence of HTLV-I Gag protein in cell culture supernatants using a p19-specific ELISA. MT-2 and HUT-102 cells expressed high levels of the HTLV-I Gag protein, p19, whereas only small amounts of p19 ($10^4$- to $10^5$-fold lower than that of MT-2 and HUT-102) were detected in the ATL-derived cell lines TL-Om1 and MT-1 (Fig. 1a, upper panel). The HTLV-I-uninfected human T-cell line MOLT-4 did not express p19 Gag protein (data not shown).

Next, the activity of NF-κB in these cell lines was determined by ELISA. All of these cells showed constitutive NF-κB activity, which was elevated compared with MOLT-4 cells (Fig. 1b). TL-Om1 cells showed the highest mean levels of NF-κB activity among the tested cell lines, although they did not express Tax or viral antigens. There was no significant difference in NF-κB activity between Tax-expressing and non-expressing HTLV-I-associated cell lines, as described [27].

### 3.2. DHMEQ inhibits NF-κB in Tax-deficient HTLV-I-associated cell lines

We evaluated the effects of DHMEQ on two HTLV-I-associated cell lines that lack Tax protein (TL-Om1 and MT-1). Morphologically, DHMEQ induced significant apoptosis as shown by deletion of cell clusters and nuclear fragmentation (Fig. 1c). After 48 h of DHMEQ treatment, Hoechst 33342 staining of nuclei showed significant apoptosis in both TL-Om1 and MT-1 cell lines (Fig. 1d). We next examined the effects of DHMEQ on the constitutive DNA binding activity of NF-κB in these cells. The cells were cultured with various concentrations of DHMEQ (0, 20 or 40 μg/ml) for 16 h (Fig. 1e). Both concentrations of DHMEQ inhibited NF-κB activation in MT-1 cells by approximately 60% compared to control cells. Likewise, DHMEQ (20 and 40 μg/ml) inhibited NF-κB activation in TL-Om1 cells by approximately 80% and 90%, respectively, compared to control cells. NF-κB p65 translocation to the nucleus was inhibited in TL-Om1 and MT-1 cells treated with DHMEQ (Fig. 1f). The relative nuclear-to-cytoplasmic ratio of p65 in TL-Om1 and MT-1 cells without DHMEQ was >3.0 and 1.5, respectively, whereas in cells treated with DHMEQ, the ratio was the same as in the HTLV-I-uninfected T-cell line, MOLT-4. These results are consisted with our previous report [9].

### 3.3. DHMEQ inhibits death in mice inoculated intraperitoneally with Tax-deficient HTLV-I-infected cell lines

To evaluate the anti-tumor effect of DHMEQ against HTLV-I-infected cell lines derived from ATL patients, intraperitoneal inoculation of NOD/SCID $\beta 2m^{null}$ mice with $5 \times 10^7$ TL-Om1 or MT-1 cells was performed. A dose of 12 mg/kg of either DHMEQ or vehicle was administrated via intraperitoneal injection on day 0 of cell inoculation and three times a week thereafter for 5 weeks. Whereas 5 of 6 (83%) DHMEQ-treated mice were alive 5 weeks after TL-Om1 inoculation, all 6 of the control (vehicle-treated) mice died by 4 weeks after cell inoculation ($P = 0.008$ by Fisher's exact test; Fig. 2a). Likewise, only 1 of 5 (20%) control mice inoculated with MT-1 survived for 5 weeks after cell inoculation, whereas all 6 of the DHMEQ-treated mice were alive at 5 weeks post-inoculation ($P = 0.015$ by Fisher's exact test; Fig. 2b).

In TL-Om1-inoculated mice, all of the six mice that received vehicle alone had visible tumors (see representative mouse Fig. 3a, left panel and Fig. 3b), whereas only two of six DHMEQ-treated mice (33%) formed small gross tumors ($P = 0.03$ by Fisher's exact test; see representative tumor-free mouse Fig. 3a, right panel and Fig. 3b). In MT-1-inoculated mice, 40% of mice treated with vehicle alone had gross tumors, whereas none of the mice treated with DHMEQ had gross tumors (Fig. 3b). To determine

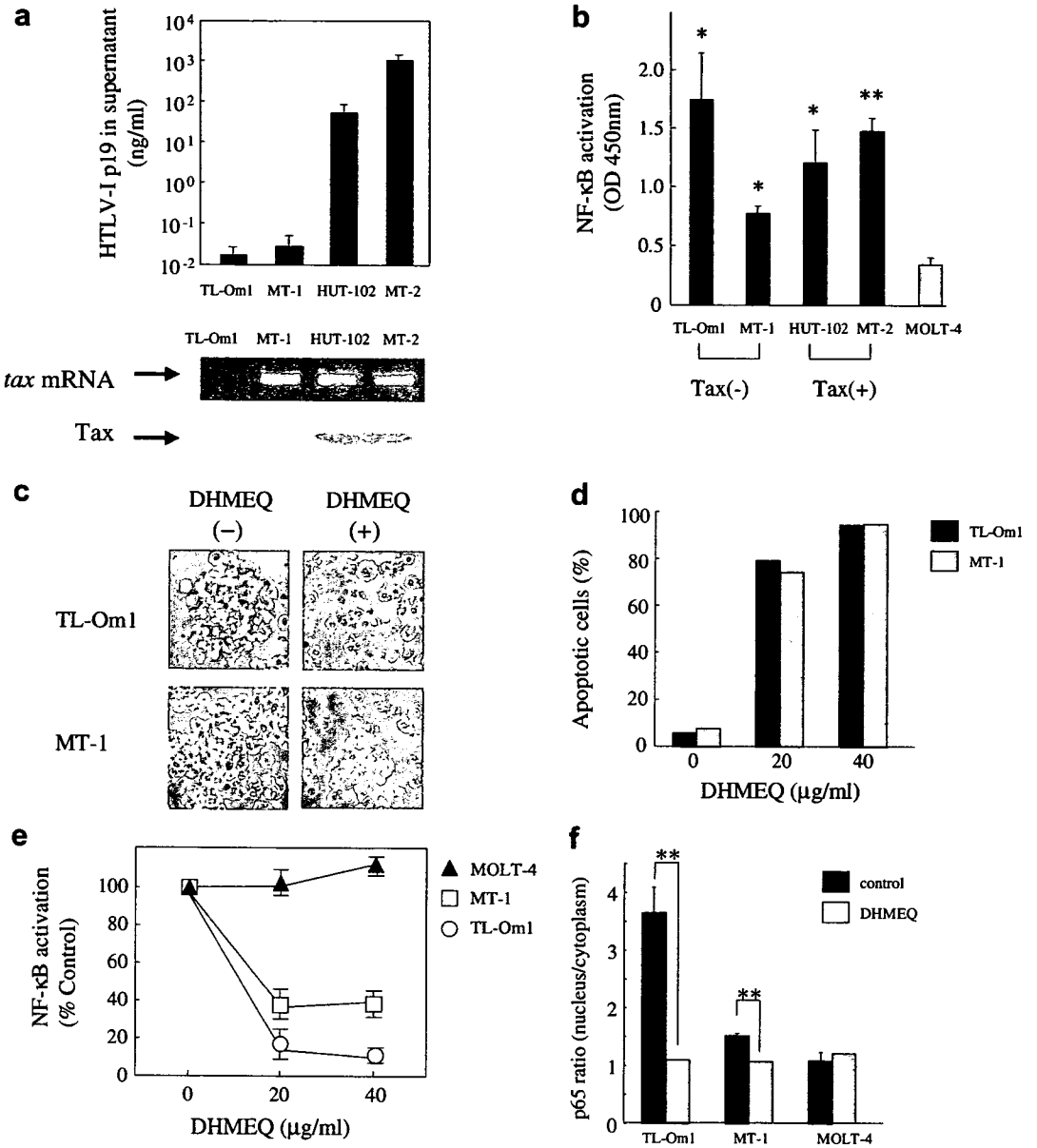


Fig. 1. Characterization of HTLV-I-associated cell lines and analysis of the effects of DHMEQ on NF-κB activity in Tax-deficient cell lines in vitro. (a) The upper panel reflects p19 Gag antigen content in culture supernatants from each cell line, as detected by ELISA. Bars represent mean values ± standard deviation (SD) of triplicate samples. The middle panel reflects Tax mRNA expression in each cell line detected by RT-PCR and the lower panel reflects Tax protein expression in each cell line detected by Western blot analysis. (b) NF-κB activity in TL-Oml, MT-1, HUT-102, MT-2 and in an uninfected cell line, MOLT-4, was measured by ELISA. This experiment was repeated three times ($n = 3$), and the data presented represent means ± SD. Statistical analysis was performed using the Student's $t$-test. $^{*}P < 0.05$, $^{**}P < 0.01$ vs. MOLT-4. (c) Morphologic examination of TL-Oml and MT-1 cells after treatment with DHMEQ using a phase contrast microscope. TL-Oml and MT-1 cells were treated with DHMEQ (20 μg/ml) for 24 h prior to analysis (magnification, 200×). (D) Induction of apoptosis of TL-Oml and MT-1 cells by DHMEQ. After 48 h of DHMEQ treatment, cells were fixed and stained with Hoechst 33342. At least 1000 stained cells were counted and assessed as apoptotic or non-apoptotic. Representative results of three independent experiments are shown. (e) DHMEQ inhibits NF-κB activity in TL-Oml and MT-1 cells. After 16 h of incubation with DHMEQ or with vehicle alone (DMSO), NF-κB activity was measured in using ELISA. MOLT-4 was used as an HTLV-I-uninfected cell control. Data are expressed as a percentage of control (vehicle-treated) activity and represent means ± SD. (f) The nuclear to cytoplasmic p65 in DHMEQ-treated cells. The results of three independent experiments are shown. Data are expressed as a percentage of control (vehicle-treated) activity and represent means ± SD. Statistical analysis was performed using the Student's $t$-test. $^{**}P < 0.01$ vs. control.

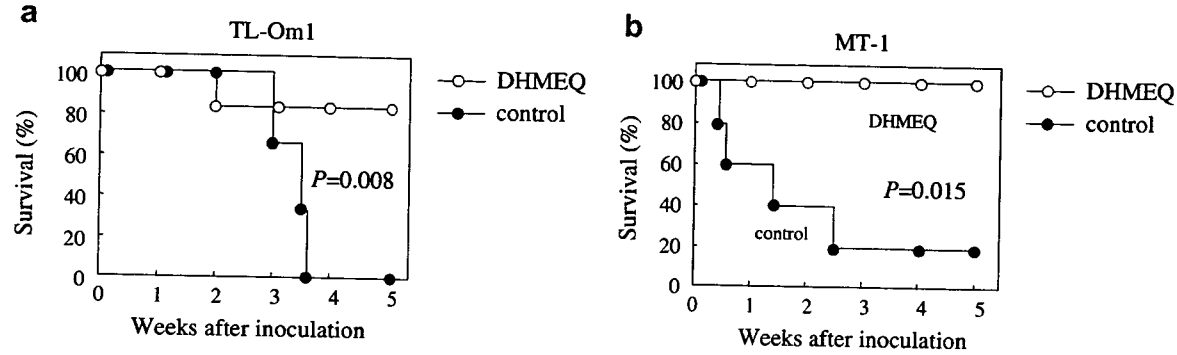


Fig. 2. DHMEQ increases survival of NOD/SCID $\beta 2m^{null}$ mice inoculated intraperitoneally with Tax-deficient HTLV-I-infected cell lines. Survival curves of mice injected with TL-Oml cells (a) or MT-1 cells (b) in the presence of DHMEQ (12 mg/kg body weight) or carboxymethyl cellulose vehicle control. The percent of DHMEQ-treated mice that survived TL-Oml or MT-1 inoculation was statistically different from that of the vehicle-treated control group. *P*, Fisher's exact test *P*-value.

whether the tumors were derived from inoculated cells, genomic DNA extracted from tumors was subjected to PCR using primers specific for the HTLV-I *tax* and human *β*-globin genes. PCR analysis showed that tumors originated from the inoculated cells (Fig. 3c).

We next compared the infiltration of inoculated cells into organs of control mice and DHMEQ-treated mice. To detect infiltration of inoculated cells into various organs, genomic DNA extracted from each organ was subjected to PCR analysis. The organs in which both HTLV-I *tax* and human *β-globin* genes were detected were considered positive (Fig. 4a). In TL-Oml inoculated mice, injected cells were present in all organ types tested from both DHMEQ-treated and untreated mice. However, the incidence of organs positive for both genes in DHMEQ-treated mice was lower than that in untreated mice. Specifically, 33% of kidneys from mice treated with DHMEQ were positive, compared with

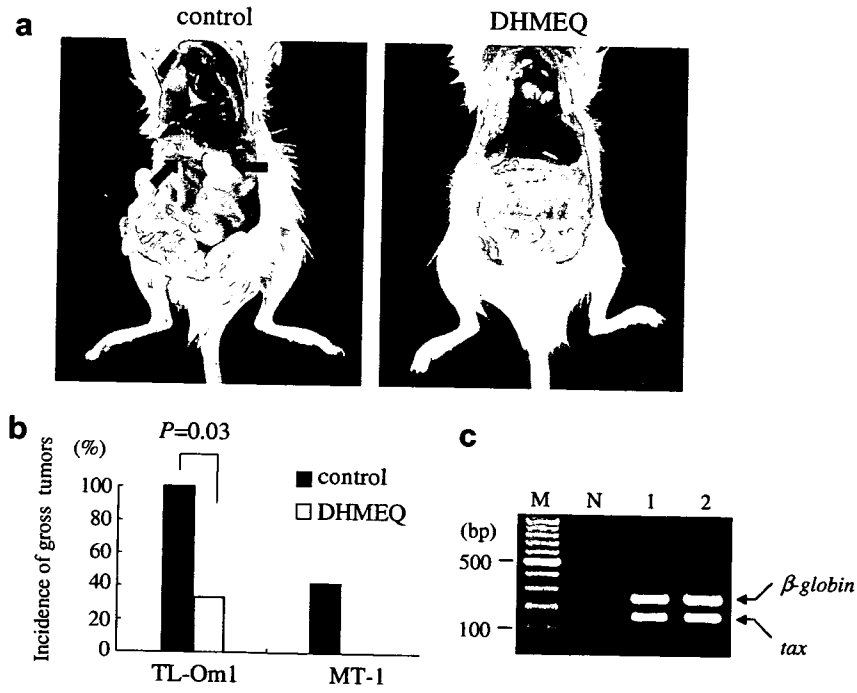


Fig. 3. DHMEQ inhibits tumor formation arising from intraperitoneal inoculation of TL-Oml or MT-1 cells in NOD/SCID $\beta 2m^{null}$ mice. (a) In TL-Oml inoculated mice, we observed gross tumor formation in the peritoneal cavity of vehicle-treated control mice (left) but not in DHMEQ treated mice (right). (b) DHMEQ reduces the incidence of gross tumors in mice inoculated with TL-Oml or MT-1 cells. *P*, Fisher's exact test *P*-value. (c) PCR analysis to detect HTLV-I *tax* (159 bp PCR product) and human *β-globin* (262 bp PCR product) was used to determine whether tumors originated from the inoculated cells. Lane 1, tumor from TL-Oml inoculated vehicle-treated mice; lane 2, tumor from MT-1 inoculated vehicle-treated mice; N, no template DNA; M, 100 bp ladder marker.

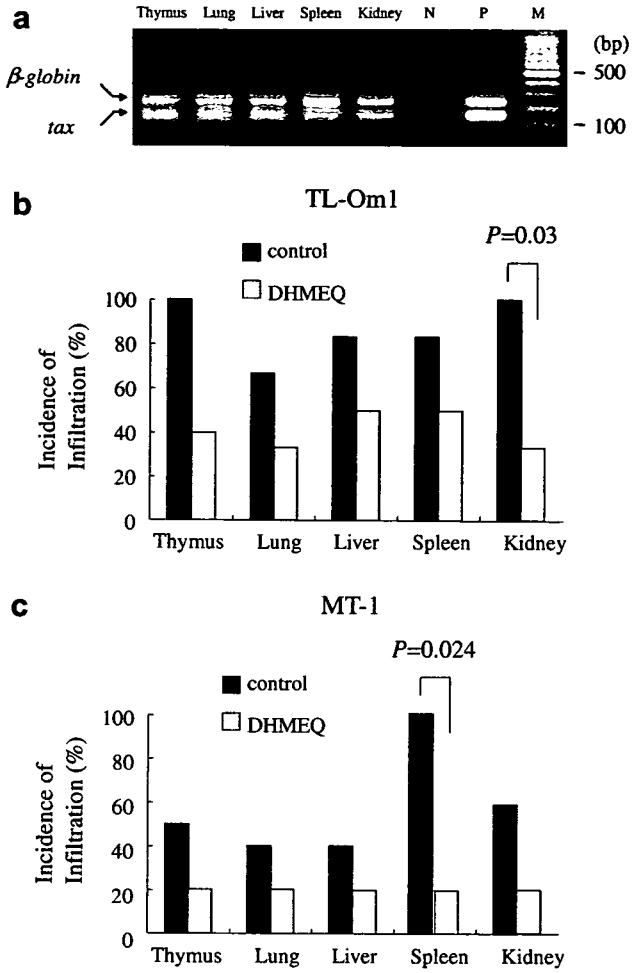


Fig. 4. PCR analysis of genomic DNA from various organs to determine infiltration of TL-Om-1 or MT-1 cells introduced by intraperitoneal inoculation in NOD/SCID β2m $^{null}$ mice treated with DHMEQ or vehicle (control). PCR primers were specific for either HTLV-I *tax* or human *β-globin*. Only those organs in which both genes were detected were considered positive. (a) Agarose gel electrophoresis of PCR reactions from a representative vehicle-treated mouse inoculated with TL-Om1 cells showing that all tested organs were positive for both genes. N, no template DNA; P, positive control from TL-Om1 cell genomic DNA; M, 100 bp ladder marker. (b and c) Graphical representation of PCR analyses indicating the infiltration of tumor cells into various organs in mice inoculated with TL-Om1 (b) or MT-1 (c) cells treated with DHMEQ or vehicle (control). *P*, Fisher's exact test *P*-value.

100% of kidneys from mice treated with vehicle alone ($P = 0.03$ by Fisher's exact test, $n = 6$ for each group; Fig. 4b).

Similarly, in MT-1 inoculated animals, the incidence of infiltrated organs in DHMEQ-treated mice was lower than that in untreated controls, although the infiltration of MT-1 cells in various organs overall was lower than that of TL-Om1 cells (Fig. 4c). Spleen infiltration was found in 20% of mice treated with DHMEQ and in 100% of mice treated with vehicle alone ($P = 0.024$ by Fisher's exact test, $n = 5$ for each group; Fig. 4c). Taken together, these data suggest that DHMEQ inhibits tumor-related death, tumor formation, and infiltration of HTLV-I-infected cells derived from ATL patients in this mouse model.

### *3.4. In vivo treatment of subcutaneous TL-Om1 tumors with DHMEQ*

We next attempted to quantitate the effect of DHMEQ on tumors from NOD/SCID β2m$^{null}$ mice in which TL-Om1 cells were introduced into the post-auricular area by subcutaneous injection. In control mice, tumors appeared 3 weeks after inoculation, and after 5 weeks they encompassed the whole area surrounding the cervical vertebrae (Fig. 5A; right). In contrast, mice treated with intraperitoneal DHMEQ injections had small tumors near the cervical vertebrae (Fig. 5A; left). Treatment with DHMEQ significantly inhibited the growth of TL-Om1 cells in vivo ($P < 0.05$ by Student's *t*-test, $n = 8$ for each

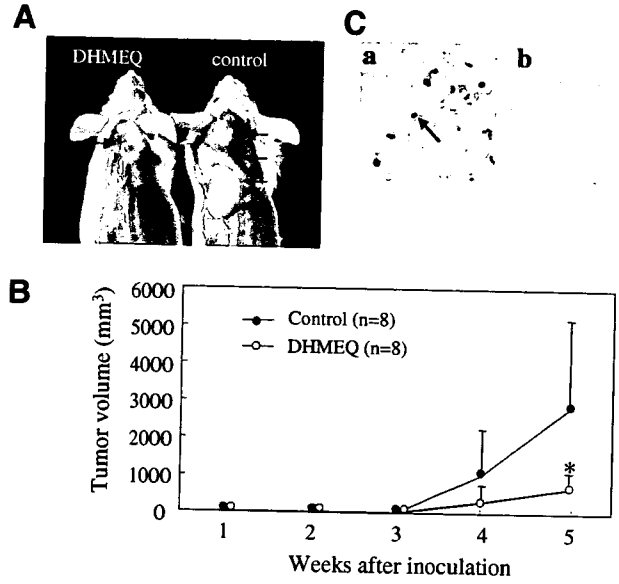


Fig. 5. DHMEQ inhibits tumor formation arising from subcutaneous inoculation of TL-Om1 in NOD/SCID $\beta 2m^{null}$ mice and increases apoptotic tumor cell death. TL-Om1 cells ($5 \times 10^7$ per mouse) were inoculated subcutaneously in the post-auricular region. Mice were treated with intraperitoneal injections of DHMEQ (12 mg/kg) or vehicle. (A) Photograph of a representative DHMEQ-treated mouse (left) and a vehicle-treated mouse (right). (B) Serial changes in tumor volume in DHMEQ- and vehicle-treated mice. Data represent means ± SD. $^*P < 0.05$ vs. control by Student's *t*-test. (C) Representative TUNEL assay showing apoptosis in gross tumors from a mouse treated with DHMEQ (a). No apoptotic cells were seen in vehicle-treated tumors (b). Original magnification, 50×.

group), and the serial changes in subcutaneous tumor volume in DHMEQ-treated and untreated mice are shown in Fig. 5B. We confirmed the inoculated cell origin of all tumors recovered from the mice using PCR primers for HTLV-I *tax* and human *β-globin* genes (data not shown). To examine the effect of DHMEQ on the induction of apoptosis in these tumors, we performed TUNEL assays on tumor tissue sections. We observed no apoptotic cells in tumors from untreated mice (Fig. 5C, panel b), whereas apoptotic cells in tumors from DHMEQ-treated mice were observed (Fig. 5C, panel a).

## 4. Discussion

Here, we have shown that Tax expression could not be detected in MT-1 cells by Western blotting, but could be detected by RT-PCR, whereas Tax expression in TL-Om1 cells was not detected by either method. These data indicate that MT-1 and TL-Om1 cell lines do in fact closely reflect the status of Tax expression found in primary leukemic cells isolated from ATL patients [28,29]. Among the cells lines tested, NF-κB activity and the nuclear translocation of p65 were the highest in TL-Om1 cells. In both TL-Om1 and MT-1 cells, DHMEQ induced apoptosis and inhibited activation of NF-κB by reducing the nuclear translocation of p65 to levels found in the HTLV-I-uninfected cell line MOLT-4. These results suggest that Tax-independent mechanisms for induction of NF-κB activation exist in these cells, and that DHMEQ inhibits both Tax-dependent and -independent mechanisms of NF-κB activity in ATL cells. In agreement with this, NF-κB inhibition by DHMEQ has been shown to down-regulate expression of genes involved in anti-apoptosis or cell cycle progression [9].

To establish the growth of the ATL-derived cell lines TL-Om1 and MT-1 in mice, we used NOD/SCID $\beta 2m^{null}$ mice – which have low NK cell activity and lack β2-microglobulin (β2 m) [23]. Mice inoculated with these cells via intraperitoneal injection showed rapid death from tumors. We demonstrated that DHMEQ also inhibited tumor formation, inhibited infiltration of inoculated cells into various organs, and reduced mortality in NOD/SCID $\beta 2m^{null}$ mice inoculated with Tax-deficient ATL-derived cell lines. It is important to note that these data resemble the effects of DHMEQ in NK-free SCID mice injected with the Tax-expressing HTLV-I-transformed cell lines MT-2 and HUT-102 [21,22] and suggest that DHMEQ may have broad application for treatment of ATL patients. We found that 100% of NOD/SCID $\beta 2m^{null}$ mice inoculated with TL-Om1 cells formed

gross tumors (defined as having a largest measured diameter of >3 mm) in the peritoneal cavity, whereas only 40% of MT-1-inoculated animals demonstrated gross tumor formation. In fact, control mice that were injected with MT-1 primarily formed very small disseminated masses, rather than gross tumors, within the peritoneal cavity. However, the origin of these masses could not be identified because we could not detect either the HTLV-I *tax* or human *β-globin* genes by PCR due to the small amount of genomic DNA available.

The TL-Om1 cell line was chosen for further analysis of the anti-tumor effects of DHMEQ because 100% of TL-Om1-inoculated NOD/SCID $\beta 2m^{null}$ mice formed gross tumors in the peritoneal cavity. We showed that DHMEQ suppressed the growth of transplanted cells in NOD/SCID $\beta 2m^{null}$ mice injected with TL-Om1 cells subcutaneously, in contrast to the significant increase in tumor burden observed in non-treated mice. Furthermore, apoptotic cells were present in tumors from DHMEQ-treated mice, similar to that reported for Tax-expressing HTLV-I-transformed cells [21]. Although mice injected subcutaneously with HUT-102 cells have been shown to form tumors at the inoculation site and have shown infiltration of inoculated cells into various organs [22], we could not detect the infiltration of TL-Om1 cells into other organs in either DHMEQ-treated or non-treated mice inoculated with TL-Om1 cells subcutaneously. This discrepancy is probably due to tumor volume at the inoculation site, because we found little difference in infiltration of these cells via intraperitoneal injection in each mouse model [21]. However, this system was useful for directly measuring response to DHMEQ in vivo and for detecting apoptosis.

In conclusion, DHMEQ significantly prevented the growth of tumors resulting from injection of Tax-deficient HTLV-I-infected cells in NOD/SCID $\beta 2m^{null}$ mice. Combined with previous studies, these results indicate that DHMEQ has strong potential for ATL therapy, regardless of whether Tax expression can be detected. In addition, our data provide a more extensive analysis of an NF-κB inhibitor predicted to act as an ATL chemotherapeutic agent in vivo than any other study to date.

## Acknowledgements

This work was supported in part by a Grant-in-Aid for Scientific Research from the Japan Society for the Promotion of Science. We thank Dr. Toru Urano for helpful discussions, Noboru Sakio and Noriyuki Sakamoto for animal care, and Yoshiteru Tanaka for technical assistance. The anti-Tax/HTLV-I Tax hybridoma 168A51-42 (Tab176) was obtained from Dr. Beatrice C. Langton through the AIDS Research and Reference Reagent Program, Division of AIDS, NIAID, NIH (Bethesda, MD).

## References

[1] B.J. Poiesz, F.W. Ruscetti, A.F. Gazdar, P.A. Bunn, J.D. Minna, R.C. Gallo, Detection and isolation of type C retrovirus particles from fresh and cultured lymphocytes of a patient with cutaneous T cell lymphoma, Proc. Natl. Acad. Sci. USA 77 (1980) 7415–7419.

[2] Y. Hinuma, K. Nagata, M. Hanaoka, M. Nakai, T. Matsumoto, K.I. Kinoshita, et al., Adult T cell leukemia: antigen in an ATL cell line and detection of antibodies to the antigen in human sera, Proc. Natl. Acad. Sci. USA 78 (1981) 6476–6480.

[3] T. Watanabe, HTLV-I-associated diseases, Int. J. Hematol. 66 (1997) 257–278.

[4] Y. Yamada, M. Tomonaga, H. Fukuda, S. Hanada, A. Utsunomiya, M. Tara, et al., A new G-CSF-supported combination chemotherapy, LSG15, for adult T-cell leukaemia-lymphoma: Japan Clinical Oncology Group Study 9303, Br. J. Haematol. 113 (2001) 375–382.

[5] S. Yamaoka, G. Courtois, C. Bessia, S.T. Whiteside, R. Weil, F. Agou, et al., Complementation cloning of NEMO, a component of the IκB kinase complex essential for NF-κB activation, Cell 93 (1998) 1231–1240.

[6] S.C. Sun, S. Yamaoka, Activation of NF-kB by HTLV-I and implications for cell transformation, Oncogene 24 (2005) 5952–5964.

[7] N. Mori, M. Fujii, S. Ikeda, Y. Yamada, M. Tomonaga, D.W. Ballard, et al., Constitutive activation of NF-κB in primary adult T cell leukemia cells, Blood 93 (1999) 2360–2368.

[8] N. Hironaka, K. Mochida, N. Mori, M. Maeda, N. Yamamoto, S. Yamaoka, Tax-independent constitutive IκB kinase activation in adult T-cell leukemia cells, Neoplasia 6 (2004) 266–278.

[9] M. Watanabe, T. Ohsugi, M. Shoda, T. Ishida, S. Aizawa, M. Maruyama-Nagai, et al., Dual targeting of transformed and untransformed HTLV-1-infected T-cells by DHMEQ, a potent and selective inhibitor of NF-κB, as a strategy for chemoprevention and therapy of adult T cell leukemia, Blood 106 (2005) 2462–2471.

[10] R. Horie, T. Watanabe, K. Umezawa, Blocking NF-κB as a potential strategy to treat adult T-cell leukemia/lymphoma, Drug News Perspect. 19 (2006) 201–209.

[11] K. Umezawa, Inhibition of tumor growth by NF-κB inhibitors, Cancer Sci. 97 (2006) 990–995.

[12] N. Matsumoto, H. Iinuma, T. Sawa, T. Takeuchi, S. Hirano, T. Yoshioka, et al., Epoxyquinomicins A, B, C and D, new antibiotics from Amycolatopsis. II. Effect on type II collagen-induced arthritis in mice, J. Antibiot. (Tokyo) 50 (1997) 906–911.

[13] N. Matsumoto, A. Ariga, S. To-e, H. Nakamura, N. Agata, S. Hirano, et al., Synthesis of NF-κB activation inhibitors

derived from epoxyquinomicin C, Bioorg. Med. Chem. Lett. 10 (2000) 865–869.
[14] A. Ariga, J. Namekawa, N. Matsumoto, J. Inoue, K. Umezawa, Inhibition of tumor necrosis factor-α-induced nuclear translocation and activation of NF-κB by dehydroxymethylepoxyquinomicin, J. Biol. Chem. 277 (2002) 24625–24630.
[15] E. Kikuchi, Y. Horiguchi, J. Nakashima, K. Kuroda, M. Oya, T. Ohigashi, et al., Suppression of hormone-refractory prostate cancer by a novel nuclear factor κB inhibitor in nude mice, Cancer Res. 63 (2003) 107–110.
[16] D.V. Starenki, H. Namba, V.A. Saenko, A. Ohtsuru, S. Maeda, K. Umezawa, et al., Induction of thyroid cancer cell apoptosis by a novel nuclear factor κB inhibitor, dehydroxymethylepoxyquinomicin, Clin. Cancer Res. 10 (2004) 6821–6829.
[17] G. Matsumoto, M. Muta, K. Umezawa, T. Suzuki, K. Misumi, K. Tsuruta, et al., Enhancement of the caspase-independent apoptotic sensitivity of pancreatic cancer cells by DHMEQ, an NF-κB inhibitor, Int. J. Oncol. 27 (2005) 1247–1255.
[18] M. Watanabe, M.Z. Dewan, T. Okamura, M. Sasaki, K. Itoh, M. Higashihara, et al., A Novel NF-κB inhibitor DHMEQ selectively targets constitutive NF-κB activity and induces apoptosis of multiple myeloma cells in vitro and in vivo, Int. J. Cancer 114 (2005) 32–38.
[19] H. Tatetsu, Y. Okuno, M. Nakamura, F. Matsuno, T. Sonoki, I. Taniguchi, et al., Dehydroxymethylepoxyquinomicin, a novel nuclear factor-κB inhibitor, induces apoptosis in multiple myeloma cells in an IκBα-independent manner, Mol. Cancer Ther. 4 (2005) 1114–1120.
[20] G. Matsumoto, J. Namekawa, M. Muta, T. Nakamura, H. Bando, K. Tohyama, et al., Targeting of nuclear factor κB pathways by dehydroxymethylepoxyquinomicin, a novel inhibitor of breast carcinomas: antitumor and antiangiogenic potential in vivo, Clin. Cancer Res. 11 (2005) 1287–1293.
[21] T. Ohsugi, R. Horie, T. Kumasaka, A. Ishida, T. Ishida, K. Yamaguchi, et al., In vivo antitumor activity of the NF-kB inhibitor dehydroxymethylepoxyquinomicin in a mouse model of adult T-cell leukemia, Carcinogenesis 26 (2005) 1382–1388.
[22] T. Ohsugi, T. Kumasaka, A. Ishida, T. Ishida, R. Horie, T. Watanabe, et al., In vitro and in vivo antitumor activity of the NF-κB inhibitor DHMEQ in the human T-cell leukemia virus type I-infected cell line, HUT-102, Leukemia Res. 30 (2006) 90–97.
[23] S.W. Christianson, D.L. Greiner, R.A. Hesselton, J.H. Leif, E.J. Wagar, I.B. Schweitzer, et al., Enhanced human CD4+ T cell engraftment in β2-microglobulin-deficient NOD-scid mice, J. Immunol. 158 (1997) 3578–3586.
[24] K. Sugamura, M. Fujii, M. Kannagi, M. Sakitani, M. Takeuchi, Y. Hinuma, Cell surface phenotypes and expression of viral antigens of various human cell lines carrying human T-cell leukemia virus, Int. J. Cancer 34 (1984) 221–228.
[25] I. Miyoshi, I. Kubonishi, S. Yoshimoto, T. Akagi, Y. Ohtsuki, Y. Shiraishi, et al., Type C virus particles in a cord T-cell line derived by co-cultivating normal human cord leukocytes and human leukaemic T-cells, Nature 294 (1981) 770–771.
[26] T. Ohsugi, K. Kumasaka, T. Urano, Construction of a full-length human T cell leukemia virus type I (HTLV-I) genome from MT-2 cells containing multiple defective proviruses using overlapping polymerase chain reaction, Anal. Biochem. 329 (2004) 281–288.
[27] Y. Satou, K. Nosaka, Y. Koya, JI. Yasunaga, S. Toyokuni, M. Matsuoka, Proteasome inhibitor, bortezomib, potently inhibits the growth of adult T-cell leukemia cells both in vivo and in vitro, Leukemia 18 (2004) 1357–1363.
[28] T. Kinoshita, M. Shimoyama, K. Tobinai, M. Ito, S. Ito, S. Ikeda, et al., Detection of mRNA for the tax1/rex1 gene of human T-cell leukemia virus type I in fresh peripheral blood mononuclear cells of adult T-cell leukemia patients and viral carriers by using the polymerase chain reaction, Proc. Natl. Acad. Sci. USA 86 (1989) 5620–5624.
[29] Y. Furukawa, M. Osame, R. Kubota, M. Tara, M. Yoshida, Human T-cell leukemia virus type-1 (HTLV-1) Tax is expressed at the same level in infected cells of HTLV-1-associated myelopathy or tropical spastic paraparesis patients as in asymptomatic carriers but at a lower level in adult T-cell leukemia cells, Blood 85 (1995) 1865–1870.

BRAIN RESEARCH 1149 (2007) 223-231

available at www.sciencedirect.com

ScienceDirect

www.elsevier.com/locate/brainres

BRAIN RESEARCH

Research Report

# Granulocyte colony-stimulating factor (G-CSF) mobilizes bone marrow-derived cells into injured spinal cord and promotes functional recovery after compression-induced spinal cord injury in mice

*Masao Koda*[a,*], *Yutaka Nishio*[a], *Takahito Kamada*[a], *Yukio Someya*[a], *Akihiko Okawa*[a], *Chisato Mori*[b], *Katsunori Yoshinaga*[c], *Seiji Okada*[d], *Hideshige Moriya*[a], *Masashi Yamazaki*[a]

[a]*Department of Orthopaedic Surgery, Chiba University, Graduate School of Medicine, 1-8-1 Inohana, Chuo-ku, Chiba 260-8670, Japan*
[b]*Department of Bioenvironmental Medicine, Chiba University, Graduate School of Medicine, Chiba, Japan*
[c]*Chiba Rehabilitation Center, Chiba, Japan*
[d]*Division of Hematopoiesis, Center for AIDS Research, Kumamoto University, Kumamoto, Japan*

ARTICLE INFO

*Article history:*
Accepted 21 February 2007
Avaialble online 1 March 2007

*Keywords:*
Granulocyte colony stimulating factor (G-CSF)
Spinal cord injury
Bone marrow-derived cell
Functional recovery

ABSTRACT

The aim of the present study was to elucidate the effects of granulocyte colony-stimulating factor (G-CSF)-mediated mobilization of bone marrow-derived stem cells on the injured spinal cord. Bone marrow cells of green fluorescent protein (GFP) transgenic mice were transplanted into lethally irradiated C57BL/6 mice. Four weeks after bone marrow transplantation, spinal cord injury was produced by a static load (20 g, 5 min) at T8 level. G-CSF (200 μg/kg/day) was injected subcutaneously for 5 days. Immunohistochemistry for GFP and cell lineage markers was performed to evaluate G-CSF-mediated mobilization of bone marrow-derived cells into injured spinal cord. Hind limb locomotor recovery was assessed for 6 weeks. Immunohistochemistry revealed that G-CSF increased the number of GFP-positive cells in injured spinal cord, indicating that bone marrow-derived cells were mobilized and migrated into injured spinal cord. The numbers of double positive cells for GFP and glial markers were larger in the G-CSF treated mice than in the control mice. Luxol Fast Blue staining revealed that G-CSF promoted white matter sparing. G-CSF treated mice showed significant recovery of hind limb function compared to that of the control mice. In conclusion, G-CSF showed efficacy for spinal cord injury treatment through mobilization of bone marrow-derived cells.



## 1. Introduction

Due to recent advances in stem cell biology, the efficacy of cell therapy for central nervous system disorders, including spinal cord injury, has been reported. Amongst various types of cells, bone marrow-derived stem cells, which include hematopoietic stem cells (HSC) and bone marrow stromal cells (BMSC), also called mesenchymal stem cells (Bacigalupo, 2004; Herzog et al.,

* *Corresponding author.* Fax: +81 43 226 2116.
E-mail address: m-koda@bb.em-net.ne.jp (M. Koda).

0006-8993/$ - see front matter © 2007 Elsevier B.V. All rights reserved.
doi:10.1016/j.brainres.2007.02.058

2003), are candidates for cell therapy of spinal cord injury, because they can be transplanted autologously. Indeed, transplantation of HSC promotes functional recovery after compression-induced spinal cord injury in mice, as we reported previously (Koshizuka et al., 2004; Koda et al., 2005), and transplantation of BMSC significantly improves hind limb function after spinal cord injury in mice and rats (Chopp et al., 2000; Hofstetter et al., 2002; Wu et al., 2003). These lines of evidence show the potential of bone marrow-derived stem cells to restore injured spinal cord tissue and to promote functional recovery.

Granulocyte colony-stimulating factor (G-CSF) is widely known as a cytokine that induces survival, proliferation and differentiation of cells of the neutrophil lineage (Nicola et al., 1983; Roberts, 2005). Further, G-CSF can mobilize bone marrow cells into peripheral blood, an action used clinically for patients with leukocytopenia and for donors of peripheral blood-derived HSCs for transplantation (Jansen et al., 2005). Bone marrow-derived stem cells mobilized by G-CSF may have the potential to migrate into and repair various injured tissues. For example, G-CSF has been shown to mobilize bone marrow-derived stem cells to repair the ischemic myocardium (Orlic et al., 2001; Kawada et al., 2004). As for the central nervous system, bone marrow cells mobilized by G-CSF migrate into, survive and express a neural phenotype in normal brain (Corti et al., 2002a), spinal cord and dorsal root ganglia (Corti et al., 2002b). Moreover, G-CSF mobilized bone marrow cells into the ischemic brain and promoted functional recovery (Kawada et al., 2006). The influence of G-CSF-mediated mobilization of bone marrow-derived stem cells on the injured spinal cord remains to be elucidated.

Here we showed that G-CSF promoted the mobilization and migration of bone marrow cells into the spinal cord, the restoration of damaged spinal cord tissue and the recovery of hind limb function.

## 2. Results

Mice tolerated the irradiation and bone marrow transplantation well. FACS analysis showed that approximately 80% of the whole bone marrow cells were positive for GFP 4 weeks after bone marrow transplantation, indicating that GFP Tg-derived bone marrow cells survived and reconstituted hematopoiesis in grafted mice (not shown).

At first, we analyzed GFP fluorescence to detect bone marrow-derived cells in the intact spinal cord. The average number of GFP-positive cells was 33.6 (16–46) per section in the PBS group and 40.3 (18–61) per section in the G-CSF group (Fig. 1D). GFP-positive cells were located mainly in the white matter and subpial zone (Figs. 1A–C). There was no significant difference between the numbers of GFP-positive cells in the PBS and G-CSF groups (Fig. 1D).

Twenty-four hours after injury, GFP-positive cells had accumulated in the lesion epicenter. Most of the GFP-positive cells in the lesioned site were round, and the remaining were spindle-shaped (Figs. 2A, D). There was no significant difference between the number of GFP-positive cells in the SCI+PBS and SCI+G-CSF groups (352.4±24.2 in the SCI+PBS group and 331.7±23.6 in the SCI+G-CSF group, Fig. 2F). Next, we performed immunohistochemistry for cell-specific markers to elucidate the phenotype of GFP-positive cells in the injured spinal cord. Twenty-four hours after injury, GFP-positive

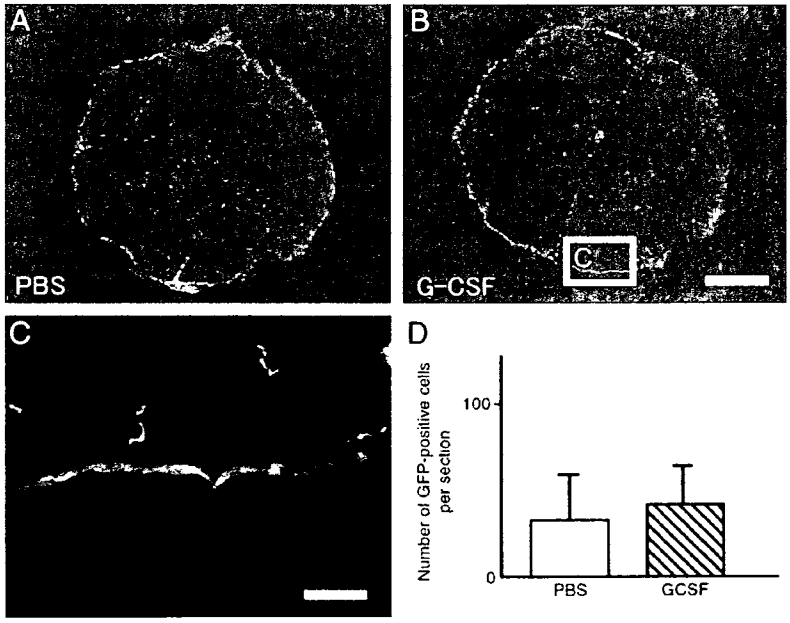


**Fig. 1 – Immunohistochemistry for GFP in normal spinal cord after PBS (A) or G-CSF (B) injection. (C) is the higher-magnification view indicated as a box in (B). There was no significant difference in the number of GFP-positive cells between the PBS and G-CSF groups (D). GFP-positive cells were located in the white matter and subpial zone (C). Bars = 500 μm (A, B) and 30 μm (C). Values are mean ± S.E.M. (D).**

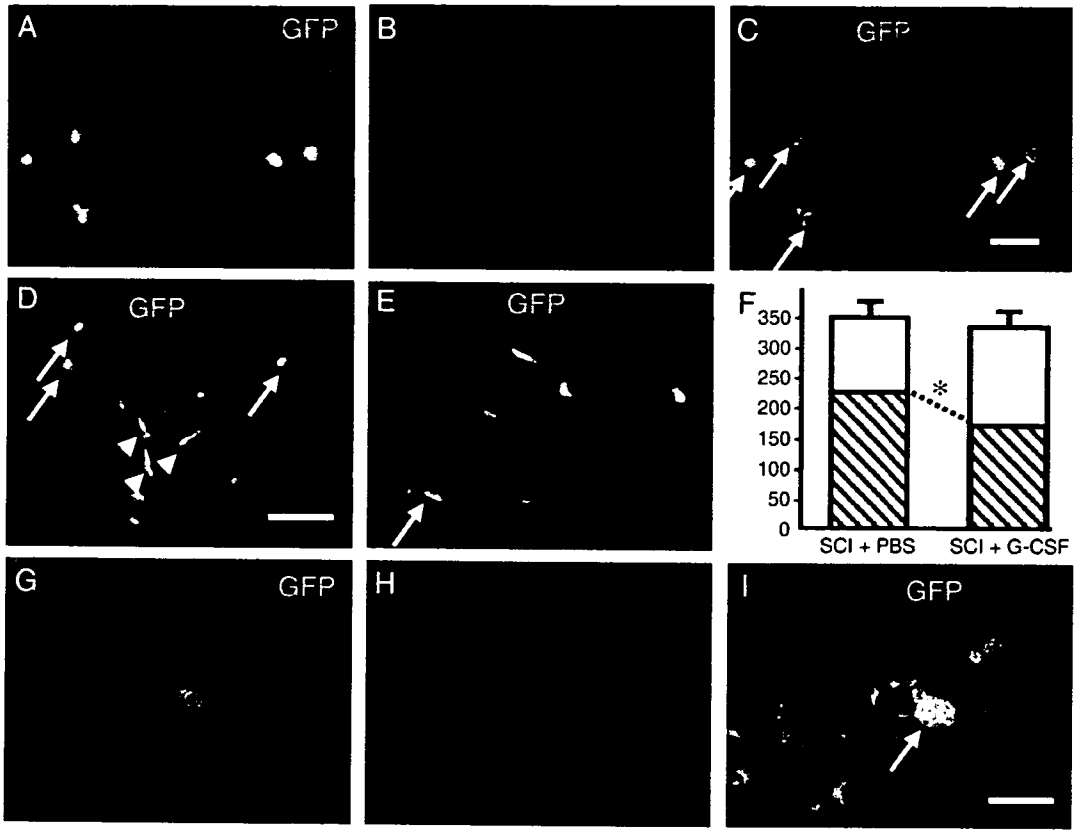


**Fig. 2 – Immunohistochemistry for GFP and cell-specific markers in the acute phase of spinal cord injury. Near the lesion epicenter, GFP-positive round cells were also positive for neutrophil antigen (A–C, D, arrows). GFP-positive spindle-shaped cells negative for neutrophil antigen were observed (D, arrowheads). Some of the GFP-positive spindle-shaped cells were positive for vimentin, a marker for cells of the mesenchymal lineage (E, arrow). There was no significant difference in the number of GFP-positive cells between the SCI+PBS and SCI+G-CSF groups (F). The number of GFP- and neutrophil-double-positive cells was smaller in the SCI+G-CSF group than in the SCI+PBS group (F, hatched column, $p<0.05$). In the SCI+G-CSF group, GFP- and CD34-double-positive cells were detected near the lesion epicenter (G–I, arrow). Bars = 50 μm (A–C), 100 μm (D, E) and 30 μm (G–I).**

round cells in the lesion epicenter were positive for neutrophil antigen (Figs. 2A–C, arrows). The number of cells double-positive for GFP and neutrophil antigen was smaller in the SCI+G-CSF group than that in the SCI+PBS group (Fig. 2F, hatched column). GFP-positive spindle-shaped cells were negative for neutrophil antigen (Fig. 2D, arrowheads). Some of the GFP-positive spindle-shaped cells were positive for vimentin, a marker for cells of the mesenchymal lineage (Fig.

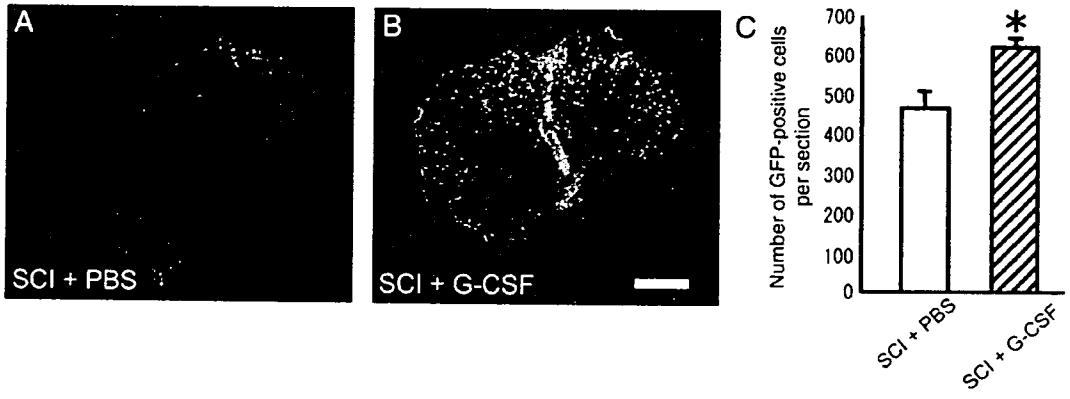


**Fig. 3 – Immunohistochemistry for GFP in the chronic phase of spinal cord injury (A: the SCI+PBS group, B: the SCI+G-CSF group). The number of GFP-positive cells was larger in the SCI+G-CSF group (C, hatched column) than that in the SCI+PBS group (C, open column). Bar = 500 μm (A, B). Values are mean ± S.E.M. and *$p<0.05$ (C).**